Synthesis and TEM investigation of PbSe and CdSe nanocrystals and nanocrystal superlattices

Joren Vos

March 2017

Supervisors:
Carlo van Overbeek
Daniël Vanmaekelbergh

Condensed Matter and Interfaces
Utrecht University

Table of contents

1. Summary 2
2. Introduction 3
3. Literature review 4
   3.1. Nanocrystals and optical properties 4
   3.2. Hot injection method 4
   3.3. Cation exchange 5
   3.4. Superstructures and self-assembly 6
      3.4.1. Self-assembly 6
      3.4.2. Forces 7
      3.4.3. Oriented attachment 8
      3.4.4. 2-D nanocrystal oriented attachment 9
4. Methodology 11
   4.1. Synthesis 11
      4.1.1. Chemicals 11
      4.1.2. Nanocrystal synthesis 11
      4.1.3. Cation exchange 12
      4.1.4. Oriented attachment 12
   4.2. Characterisation 13
      4.2.1. Absorption spectroscopy 13
      4.2.2. ICP-OES 13
      4.2.3. Transmission electron miscroscopy & energy-dispersive X-ray spectroscopy 13
5. Results and discussion 14
   5.1. PbSe nanocrystal synthesis 14
   5.2. Cation exchange 16
   5.3. Oriented attachment 18
      5.3.1. Reaction conditions 18
      5.3.2. PbSe oriented attachment results 30
      5.3.3. PbSe/CdSe oriented attachment results 37
6. Conclusions 45
7. Outlook 46
8. Acknowledgements 47

Bibliography 48

9. Appendices 52
   Appendix A: Details of the nanocrystals mentioned in this thesis 52
   Appendix B: Determination of crystal facets using electron diffraction 52

1. Summary

It has been shown before that semiconductor nanocrystals can perform oriented attachment. Since there is not much insight in the oriented attachment process and especially in why some nanocrystals do perform oriented attachment whereas others do not, oriented attachment experiments with PbSe and CdSe nanocrystals have been performed. By controlling different reaction conditions, multiple superstructures were found using PbSe nanocrystals, e.g. square, honeycomb, linear and zigzag superstructures. A way to reproducibly synthesise honeycomb superstructures has been found as well, by solving the nanocrystals in a larger toluene volume, slowing the evaporation. By performing oriented attachment experiments with mixtures of PbSe and CdSe, it was found that the CdSe nanocrystals will not be incorporated in the superstructures formed by the PbSe, but that they will be positioned close to those superstructures.

2. Introduction

When one of the dimensions of a material is reduced to nanometre scales, the material is called a nanomaterial. These materials have different optical and electronical properties than bulk product of the same material. This means that compared to the bulk product, the colour and the conductivity change. Quantum dots are made of semiconductor nanomaterials. The mentioned properties can be tuned by adjusting the size and shape of these nanocrystals.[1] Since for this research the crystallographic properties are of interest instead of the optical properties, from here on, quantum dots will be referred to as nanocrystals.

In 1998, researchers found some results which they could not explain via classical growth mechanisms, leading to the discovery of oriented attachment.[2] It was shown that microscopic crystallites can perform oriented attachment and form so-called superstructures. In this process, the particles rotate and attach to form parallel orientations in three dimensions.

In 2005 it was found that oriented attachment was shown to be useful as preparation tool for semiconductor nanocrystal structures.[3] Nanocrystals can according to this principle connect via atomic bonds at specific facets. They form superstructures which consist of a single crystal. These superstructures often have a height of a single quantum dot and can thus be seen as two-dimensional (2-D structures). The superstructures are quantum confined in the z-direction, but not in the x- and y-direction, which means that an electrical current can flow in these directions. This makes it for example possible to make transistors out of these material which are extremely efficient, since they have a lower resistance than currently used silica transistors. Furthermore, a high vacuum is not needed in the process of creating these transistors, whereas it is needed for the making of conventional silica transistors.[4]

It is however not yet possible to successfully synthesise all kinds of superstructures, the successfulness depends on the used nanocrystals. Honeycomb ordered superstructures are reported to have been made[5,6] as well as square nanosheets[5] made out PbSe nanocrystals. Oriented attachment with CdSe nanocrystals however is unsuccessful, the dots do not attach to each other. They do however perform self-assembly, forming ordered un-attached structures.

It is still unclear why the attachment with CdSe nanocrystals fails. It is also unclear which forces play a role in the attachment procedure. To understand these phenomena, further knowledge into the oriented attachment process is needed. This will help improving the synthesis of superstructures. When the synthesis of superstructures is successful and reliable, they can be used in various applications, such as the aforementioned transistors.

Therefore, the goal of this research is to get more insight in the oriented attachment process. PbSe square superstructures will be made, as these can successfully be synthesised. Cation exchange will be done on PbSe particles to obtain CdSe particles of the same size, which will be used for oriented attachment of PbSe and CdSe mixtures.

3. Literature review

3.1. Nanocrystals & optical properties

Nanocrystals are nanoparticles, made of semiconductor materials, which have a diameter of 1-100 nm. The core of the quantum dot consists of an inorganic crystal, which is stabilised by a shell of ligands (usually made from organic materials), which provides the quantum dot with chemical and colloidal stability.

These nanocrystals exhibit different optical and electronic properties than bulk counterparts of the same material. There are two factors that contribute to these properties: the large volume-to-surface ratio and the quantum confinement effects. The large volume-to-surface ratio makes the nanocrystals relatively unstable, because there are a lot of dangling bonds on the quantum dot surface. It also changes some chemical properties, they have for example a lower melting point and are more reactive than the bulk material.[7]

The inorganic core is stabilised by surrounding organic capping ligands. There are a number of ligands that can be used for stabilising the nanocrystals, such as oleic acid (OA) or trioctylphosphine (TOP). Properties like the conductivity, reactivity and stability are influenced by the capping ligands.

It has been mentioned before that a nanocrystal is an inorganic core, capped with organic ligands. The optoelectronic properties of the nanocrystal are defined by the ligands and the inorganic core, whereas the magnetic properties are defined by the inorganic core, which can for example exist of PbSe or CdSe. The properties change by changing the size and morphology of the dots by virtue of the quantum confinement effect.[8,9] This confinement is an effect that occurs when the size of the nanocrystal approaches the bulk semiconductor Bohr radius. As a result the band gap energy undergoes a blue shift and an increase in excitonic transition energy.

3.2. Hot injection method

The standard procedure to synthesise nanocrystals is the hot injection method as first described by Murray *et al.*[10] The method is based on the classical nucleation theory.[11] Hot injection is suitable for making monodisperse nanocrystals, because it separates the nucleation and growth stages. The size and shape of the synthesised nanocrystals can be tuned by adjusting the hot injection method.

There are three steps in the hot injection method. The first step is the induction period. In preparation of this step, a metal-ligand precursor is synthesised, which is heated to a high temperature. The induction period starts as soon as a chalcogenide precursor is added rapidly to the solution at a high temperature (180 °C).[12]

After the induction period, the nucleation stage starts, in which a cluster of nanoparticles is formed (the nuclei). There are two ways to end the nucleation and start the third stage, the growth stage. The first way is by lowering the concentration of free precursor in the solution, bringing it below the concentration of supersaturation, which ends the nucleation automatically. The other way is by inducing a temperature drop, thereby also terminate the nucleation process.

After the nucleation step, the growth stage starts. In this stage, the nanocrystals grow to the desired size. The growth can be controlled by manipulating certain conditions, such as the temperature, solution volume and the monomer concentration. The growth stage is quenched by the rapid injection of a polar solvent with a high boiling point (at least 150 °C) like butanol, which cools the reaction solution down, effectively stopping the reaction.

After the hot injection is finished, the product is washed with a polar solvent, centrifuged and decanted to remove any precursors, ligands and solvent, which stay in the polar supernatant. Some ligands which are already bound to the nanocrystals are removed as well, which decreases the stability of the nanocrystals.[13] The nanocrystals are at the bottom of the vial and are dissolved in an apolar solvent like hexane of toluene.

The size of the nanocrystal is dependent on the length of the growth step and the monomer concentration. By changing this length, the size can thus be fine-tuned. Nanocrystals with a size of around 5 nm are synthesised by quenching after 20 seconds. Quenching after a minute leads to nanocrystals with a size of 10 nm.

3.3. Cation exchange

With the hot injection method, it is possible to synthesise different nanocrystals, depending on the used precursors and the reaction conditions. However, it is often very difficult or even impossible to synthesise nanocrystals of the same size and shape that consist of different inorganic cores. In this case, cation exchange can be used.

Using cation exchange[14,15,16], it is possible to replace the cations of a product with another cation. The size, shape and morphology is the same for the two products, because the anionic framework is kept intact.

Cation exchange can be performed on nanocrystals and is a very useful tool to obtain nanocrystals made of different inorganic cores with the same size, shape and morphology. Because it is very hard or even impossible to realise this via the hot injection method, cation exchange is a powerful tool in the synthesis of nanocrystals. Cation exchange is used after the synthesis of the nanocrystals.

To perform cation exchange, an excess of the new cations should be used to ensure that a maximum number of cations is exchanged, since the reaction is not irreversible, but has an equilibrium. Furthermore, the temperature should be high to ensure that the equilibrium favours the cation exchanged products. The cations will be dissolved together with the old nanocrystals. The cations will take the place of the old cations, as they diffuse out of the crystal. This gives the following overall reaction:

$$AM + B^{2+} \leftrightarrow BM + A^{2+} \tag{2.4}$$

With A and B as bivalent metal ions and M the anion in this case.

Cation exchange will be more successful if the cation that will be exchanged is solvated more easily than the new cation in the solution.[17] There are thus two ways in which the cation exchange reaction can be favoured towards exchanging the original cation for the new one. The first way via which the cation exchange can be controlled is by using a large excess of the new cation. This gives a greater change of exchange. The second way is by using a solvent in which the original cation dissolves easily, since this will make it energetically favourable to

perform cation exchange. This is because if the original cation is dissolved easily, it will have a lower change to react back into the nanocrystal, thereby shifting the equilibrium towards the cation exchanged product.

Evers *et al.*[5] have also shown that it is possible to perform cation exchange on superstructures. Using this method, superstructures of nanocrystals that cannot be directly synthesised can still be synthesised.

3.4. Superstructures & self-assembly

Nanocrystals can perform self-assembly and form superstructures. These superstructures for example are made by drying the nanocrystal solutions, creating a meta-material.[18,19] However, these superstructures do not have interatomical connections, which means that they show no electronic coupling, meaning that there is no conductivity through the superstructure.

This is where oriented attachment comes into place. Oriented attachment was discovered in 1998, when Penn *et al.* could not explain their results via the classical growth mechanisms.[2] In this process single nanocrystals bind to each other, creating a single supercrystal. When this is combined with self-assembly, superstructures that are atomically aligned and connected can be created.

3.4.1. Self-assembly

Self-assembly is the spontaneous process where single crystallites self-organise in larger ordered structured materials. This happens when a colloidally stable solution of nanocrystals is destabilised, which can be done via solvent evaporation on a liquid surface like ethylene glycol. There is not a single superstructure that can be made, all kinds of superstructures can be made, from 1D, to 3D superstructures. They can also be built from a single type of nanocrystal or from different kinds of nanocrystals (Figure 3-1). As can be seen, the nanocrystals do not have to be of the same size. They are however not directly connected to each other, since they are separated by their ligands.[20,21,22,23]

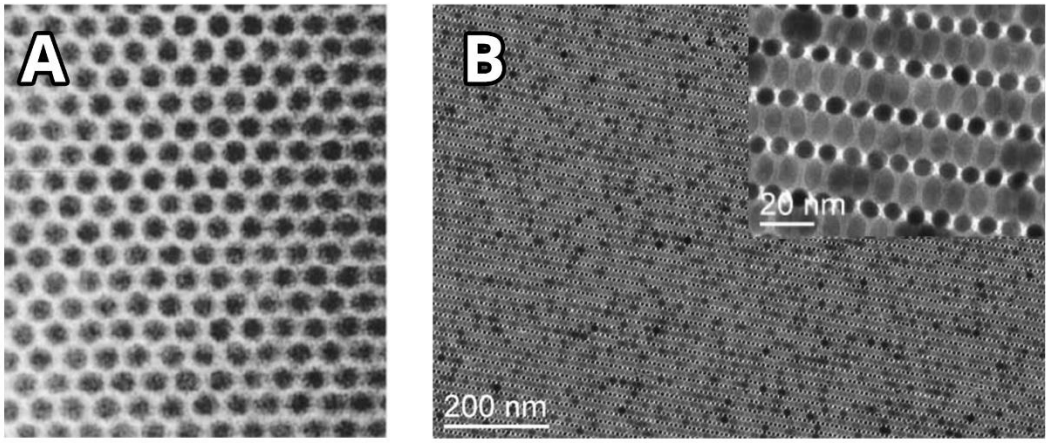

Figure 3-1: Self-assembled structures made of nanocrystals of one kind. Image adapted from Murray et al.[19] *b) Self-assembled superstructures made of different kinds of nanocrystals. Image adapted from Dong et al.*[18]

The hard sphere model can be used to explain this formation of superlattices, as the nanocrystals behave as hard spheres. Since the local free space for every nanocrystal increases in the case of the ordered system compared to the disordered system, there is an increase in entropy[20]. The model also predicts close-packed superstructures.[24] The structures found using semiconductor nanocrystals at higher temperatures match with the predictions made by this model. At low temperatures, structures can be formed that are not stable for hard spheres.[24] However, the model cannot explain results found with metal nanocrystals and the results at low temperatures, so there must be other interactions that play a role as well.[20]

3.4.2. Forces

There has been lots of research on the forces that play a role in the self-assembly and oriented attachment processes as important for this research[25,26,27]. However, it is still not clear what forces play a role in these processes and what kind of role they play. Multiple researches have shown different forces to play a role. However, there are some problems with each type of forces. Therefore, each force that might play a role in the process will be discussed below.

Surface adsorption is one of the forces that has been named, in theoretical[28,29] and experimental[30,31] research for the self-assembly of nanocrystals. The problems with surface adsorption lie in that assumptions made for the calculations are imperfect. In the research conducted by Thapar *et al.*[29] for example, there are constraints with regard to the immersion depth and the polar angle of a particle, since these are assumed on the basis of the values of the equilibrium adsorption configurations. There is also some debate on how the surface adsorption of nanocrystals actually can contribute to the formation of superstructures, since for example nanocrystals do not have well-defined surface facets.

Dipolar interactions is another force that has been named to play a role in the assembly and oriented attachment processes[3,32], which has been researched as well[33,34]. Most of these interactions stem from the result of the chalcogenide or metal on the outer facets. The problem with dipolar interactions is that there is monolayer assembly before the nanocrystals are orientated. Furthermore, it cannot explain why there is no attachment in solution.

The last force that has been named for self-assembly is the interaction with the ligands, in theory[35,36] and in experimental research[37,38]. The problem with ligand interactions is that it is very hard to model them correctly. However, they do seem to be a promising candidate, since it is already known that the ligands change the stability and reactivity of the nanocrystals. More research should been done, since the foundation has been laid for describing dense arrangements of dephormable spheres and it is anticipated that the found results also apply to other deformable objects.[35]

The main force in oriented attachment is readily acknowledged. Oriented attachment occurs at the surface of a liquid, thereby decreasing the surface area and the crystal surface facet energy. Sterical hindrance of the ligands is a problem, so they must be at least partially removed to let the attractive interactions become dominant. There are however more forces that play a role only in the oriented attachment process, since oriented attachment does not work for all semiconductor nanocrystals, they will only self-assemble. These forces are not well understood, as different research shows different forces playing a role.

3.4.3. Oriented attachment

The growth of bulk crustals happens mostly via monomer addition. However, in 1998 Penn *et al* found results which they could not explain with their knowledge about classical growth.[39,2] They therefore explained their findings by what they called 'oriented attachment'. Oriented attachment is the process in which nanocrystals attach into a single larger crystal.[40] The process is always accompanied by some Ostwald ripening, which smoothens the surface.[41]

When oriented attachment takes place, a multitude of different superstructures can be made, such as zigzag nanowires[3], chains[42], rods[43] and multipods[44].

To let nanocrystals undergo oriented attachment, ligands or solvent molecules need to be removed from the surface of the nanocrystals. There are two ways to do this, the first method is evaporation driven (for example the evaporation of the solvent). The second method is destabilisation driven, for example by addition of an anti-solvent.[45]

After the removal of the ligands and solvent molecules, attachment takes place. There are two collision mechanisms which can take place, depeding on the colloidal state of the nanocrystal suspension.[46] In the first mechanism, nanocrystals can only attach when their orientations are already the same when they collide. In the second mechanism the nanocrystals will rotate after colliding, attaching afterwards. These mechanisms are shown in Figure 3-2.

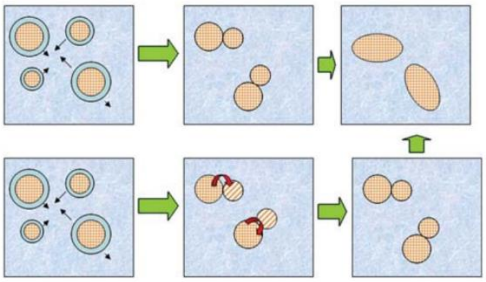

Figure 3-2: The two oriented attachments mechanisms. On top, the oriented attachment mechanism where nanocrystals must have the same orientation when they collide to attach and at the bottom, the oriented attachment mechanism where the nanocrystals collide, rotate to the same orientation and then attach. Figure adapted from Dalmaschio et al.[46]

When the nanocrystals are in dispersion and in a kinetically stable state, oriented attachment can be performed by collisions that have virtually identical orientations in their crystallography. Because the nanocrystals have a high Brownian motion in dispersion, they undergo many collisions. This means that theoretically, by maximising the number of collisions, oriented attachment should be made more successful and that oriented attachment can be described statistically. However, not all of those collisions are effective and will lead to the nanocrystals attaching to each other. This only happens when their crystallographic orientation is the same. Otherwise, they will collide, but repel each other, staying single nanocrystals.

The interactions between nanocrystals in solution are very attractive. This means that the collisions that occur cannot be described statistically. It has been shown that the nanocrystals move via translational and rotational motion.[47] Due to the attraction between the nanocrystals, this motion is increased. Finding a lattice match, the nanocrystals perform oriented attachment by attaching at a contact point (a facet). Afterwards, there is some ion-by-ion addition around the attached nanocrystals called necking.

In practice, it has been shown that oriented attachment will only take place when carried out on a substrate like ethylene glycol.[5,41]

3.4.4. 2-D nanocrystal oriented attachment

Using semiconductor materials like PbSe, it is possible to synthesise 2-D nanocrystal superstructures such as square PbSe and honeycomb PbSe via self-assembly and oriented attachment (see Figure 3-3)[5]

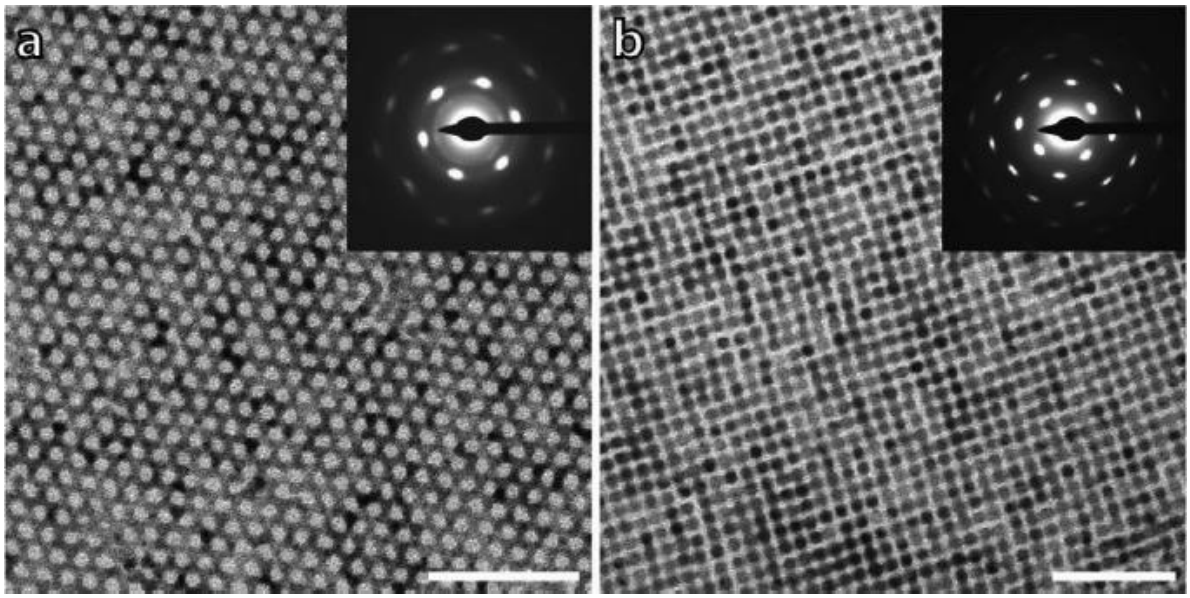

Figure 3-3: a. Honeycomb PbSe realised via self-assembly and oriented attachment. b. Square PbSe realised via self-assembly and oriented attachment. Image adapted from Evers et al.[5]

The nanocrystal made via oriented attachment grows in time, which decreases its velocity. This means that the oriented attachment slows down. Ostwald ripening however will continue[41], allowing further growth of the crystal and better connection between the single nanocrystals.

The resulting superstructures have a thickness of one nanocrystal, they can be considered as 2-D. There are different structures that can be formed via this route, such as square and honeycomb superstructures. Other researchers have shown that it is also possible to synthesise superstructures made out of octapods.[48]

In the case of oriented attachment in square superstructures, the PbSe nanocrystals will adsorb to the liquid-gas interface after which the nanocrystals self-organise[49] like a hexagonal square. They will however not have positional order in the long-range or atomic orientation. In time, a complete monolayer forms at the surface. Later, the nanocrystals will form a square structure. The <100> direction will point upwards and there will be orientation order in the 2-D direction of the superstructure.

The resulting superstructures can have interesting opto-electronic properties. For example, when the nanocrystals are ordered in a honeycomb structure[5,6], the resulting superstructure has a similar topology as graphene and the electronical properties of the single nanocrystal it was made out of.

For as of now unknown reasons, oriented attachment via the described procedure will not be successful for every kind of semiconductor nanomaterials, it is for example not possible to synthesise CdSe superstructures via oriented attachment. When this is tried, the CdSe nanocrystals will self-assemble, but not perform oriented attachment. This might be the case because of the bulk melting temperature of CdSe, which is higher than for PbSe, which will readily perform oriented attachment after self-assembly, indicating that there might be some melting process that plays a role in the process. Forces like the dipole moment might also play a role in this process.

4. Methodology

4.1. Synthesis

4.1.1. Chemicals

In the table, the chemicals used in this thesis, their abbreviation (if used), their purity and the company where they are bought are listed.

Chemical	**Abbrevation**	**Purity**	**Company**
Lead(II) acetate trihydrate	$Pb(AcO)_2 \cdot 3H_2O$	99.99%	Aldrich
Oleic Acid	OA	90%	Aldrich
Ehtylene Glycol	EG	99.8%	Aldrich
Toluene	-	99.8%	Aldrich
1-Butanol	BuOH	99.8%	Aldrich
Methanol	MeOH	99.8%	Aldrich
1-Octadecene	ODE	Technical grade 98%	Aldrich
Trioctylphosphine	TOP	90%	Aldrich
Diphenylphosphine	DPP	98%	Aldrich
Selenium Powder	Se	99.999%	Brunschwig
Tetrachloroethylene	TCE	≥99%	Aldrich
Cadmium(II) acetate dihydrate	$Cd(AcO)_2 \cdot H_2O$	98%	Aldrich
Hydrochloric Acid	-	36.5-38%	Aldrich
Nitric Acid	-	≥65%	Aldrich

4.1.2. Nanocrystal synthesis

PbSe nanocrystals were synthesised using the hot injection technique described in the theory.[10] Every step was done in an oxygen- and water free environment. A lead precursor was synthesised on a schlenk line. 39.75g ODE, 10.35g OA and 4.77g $Pb(AcO)_2 \cdot 3H_2O$ were combined in a 100 mL Erlenmeyer. This was put under vacuum and heated to 140 ˚C while stirring. The system was then left overnight under vacuum, during which the lead acetate reacted with the oleic acid, creating lead oleate. The water and acetate evaporated out of the solution. It was then stored in a nitrogen-purged glovebox.

A selenium precursor was synthesised by combining 46.59 mL TOP, 0.41 mL DPP and 3.52g Se powder in a 50 mL Erlenmeyer. This was heated to ~100 ˚C in a glovebox and stirred continuously. The selenium precursor was then stored in a glovebox at room temperature.

The hot injection was carried out in the following way. The synthesis was done in a glovebox. 19,5 mL of lead oleate was heated in a 100 mL round bottom flask. At 180 ˚C, 15 mL of the selenium precursor was swiftly added. The solution then turned brown-black. After the injection of the selenium precursor, the nanocrystals were allowed to enter the growth by keeping the temperature around 150 ˚C. The reaction was quenched after 30s with 15 mL BuOH. After 10 minutes, 10 mL MeOH was added. The product is then purified twice by the addition of methanol, centrifugation at 1183g for 5 minutes in a Hettich Rotina 38 centrifuge

and decantation, where the residue is kept. Finally, the product is dissolved in toluene and stored in a glovebox. The analysis of the product is described in section 5.1.

4.1.3. Cation exchange

To obtain CdSe nanocrystals of the same size as the synthesised PbSe nanocrystals, cation exchange was done based on the work by Casavola et al., Pietryga et al. and Evers et al.[16,50,5]

First, a cadmium precursor is synthesised. 1.15g $Cd(AcO)_2 \cdot H_2O$ and 5,56g OA are dissolved in 50 mL ODE. This was put under vacuum on a Schlenk line and heated to 140 ˚C while stirring. The system was then left overnight under these circumstances. The precursor was then stored in a glovebox.

PbSe nanocrystals were concentrated by evaporating the toluene in the antechamber of a glovebox under reduced pressure. The nanocrystals were then dissolved in 5 mL 1-octadecene and heated to 100 ˚C while stirring, together with the cadmium precursor. When the temperature was roughly 85 ˚C, the cadmium precursor was added. There was enough precursor added to have roughly 4 Cd atoms per Pb atom, estimated by a calculation dependent on the size of a spherical PbSe nanocrystal, to achieve a surplus of Cd atoms.

The solution was then further heated to 150 ˚C, where it was left for 1.45 hours. Then, the temperature was heated to 170 ˚C for half an hour. Afterwards, the solution was allowed to cool to room temperature. Then, the product is purified twice by addition of methanol, centrifugation at 143.1g for 10 minutes in a Hettich Rotina 38 centrifuge and decantation. The product is dissolved in toluene, analysed as described in section 5.2 and stored in a glovebox.

4.1.4. Oriented attachment

Oriented attachment experiments have been done based on the work done by Evers et al.[5] and Boneschanscher et al.[6] Petridishes made of glass with a diameter of 29 mm were filled with 6.5 mL EG. The temperature was set to 20 ˚C using a hot plate. 350 µL of nanocrystal solution with a solution of around 0.5 µmole/L was dropcasted to the EG.

The liquid surface of the attachment experiments was scooped with a carbon coated copper TEM grids coated with Formvar/Carbon bought at Van Loenen Instruments after the oriented attachment process. The grids were put under vacuum in the large antechamber of the glovebox and left overnight to let the EG evaporate.

There are many reaction conditions that can influence the oriented attachment process. Because of this, precautions were made to keep the conditions as stable as possible (except the specific conditions that were varied during the experiment). This means that all the experiments were done in a glove box environment with an oxygen level of 0.0 ppm and a water level <10 ppm. Also, it has been tried to keep variables like the petridish size the same and the procedure has been followed as close as possible to eliminate the effects of these conditions on the oriented attachment results. Using these precautions, the reliability and reproducibility of the process was as high as possible.

To change the oriented attachment results, multiple variations were tried in the oriented attachment, such as adding OA to the EG, adding lead oleate to the nanocrystal solution and increasing the toluene vapor pressure. These results will be discussed in the section Results.

4.2. Characterisation

4.2.1. Absorption spectroscopy

Absorption spectroscopy was done to determine the size of nanocrystals.[51] Measurements were done using a Perkin Elmer Lambda 950 UV/Vis/IR absorption spectrophotometer. Before measurements could be done, the toluene was evaporated under vacuum in the small antechamber of a glovebox and because toluene gives a peak in the same region as the nanocrystals, they were dissolved in tetrachloroethylene.

4.2.2. ICP-OES

ICP-OES experiments using a Perkin Elmer Optima 8300 ICP-OES spectrometer were done to analyse the concentration of the synthesised nanoparticles and to determine the successfulness of the cation exchange of PbSe into CdSe nanocrystals. This was done by measuring the amount of Pb and Cd. The nanocrystals were dried by evaporation in the small antechamber of a glovebox and the nanocrystals were destroyed in aqua regia and diluted in 5 volume percent acetic acid. As a baseline, stock solutions containing 5 percent of acetic acid and a 0 ppm – 1 ppm range of standard solutions, containing Cd and Pb atoms, were used.

4.2.3. Transmission electron miscroscopy & energy-dispersive X-ray spectroscopy

Images of the nanocrystals and superlattices were made using Transmission electron microscopy analyses. These images were made using a Philips Tecnai 10 and Tecnai 12 (FEI company) electron microscope. The analyses were done with an accelerating voltage of 100 of 120 kV. Diffraction was also done using these microscopes.

High Resolution Transmission Electron Microscopy and Electron Diffractive X-ray analysis, to determine the atom ratios, were done using a FEI Talos F200X electron microscope, with an accelerating voltage of 200 kV. Atom-specific analysis was also done using this Electron microscope.

5. Results and discussion

This chapter will present and discuss the results obtained during this Master's thesis. The results will be split in different parts. First, the synthesis and characterisation of PbSe nanocrystals will be discussed. This will be followed by a discussion about the cation exchange of PbSe into CdSe and the characterisation of these nanocrystals. The last part will discuss the oriented attachment of mixed PbSe and CdSe nanocrystals.

5.1. PbSe nanocrystal synthesis

Using the method explained in section 4.1.2, PbSe nanocrystals have been synthesised. The synthesis was not successful, starshaped polydisperse particles with sizes up to 10 nm were formed, which can be seen using TEM picture (see Figure 5-1).

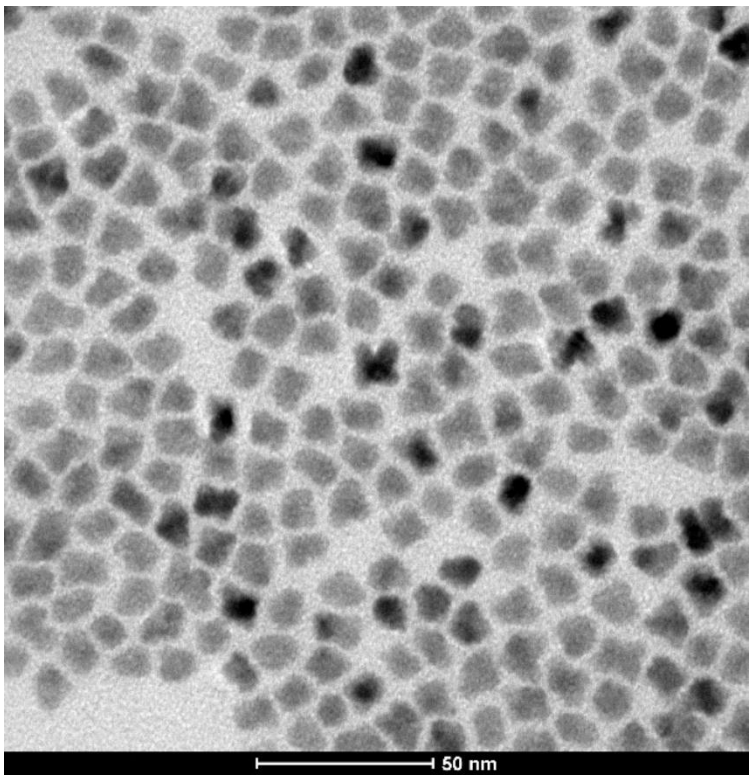

Figure 5-1: Star-shaped PbSe nanocrystals synthesised using PbSe nanocrystals synthesised via hot injection

This is also visible in the absorption spectrum, which shows no clear peak (see Figure 5-2). The reason that the particles are starshaped is that there was residual acetate in the lead oleate used in the synthesis. This is a result from insufficient degassing, probably due to a pump that is too weak. The acetate blocks the <111> surfaces and growth happens mostly on the <100> surfaces, leading to starshaped nanocrystals.[52]

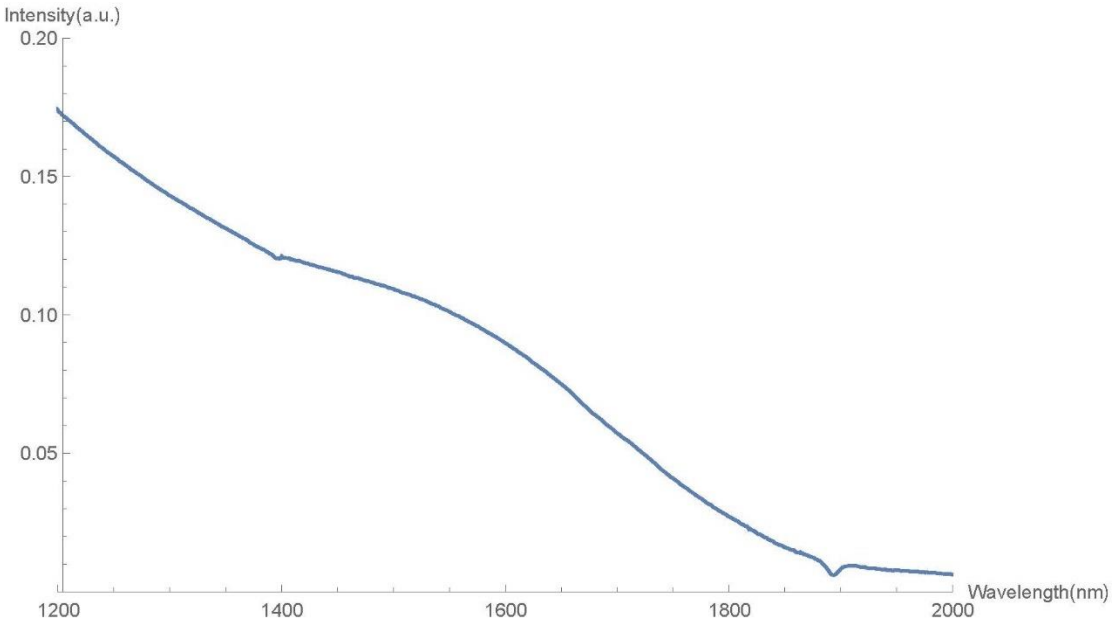

Figure 5-2: UV-VIS absorption spectrum of the star-shaped PbSe nanocrystals, shown in Figure 5-1. The spectrum is flattened and does not contain a peak, as is expected for spherical PbSe nanocrystals.

Nanocrystals made by Joep Peters were used for this research, since there was not enough time to improve the hot injection process and synthesise better nanocrystals. Using a TEM picture (Figure 5-3) and an absorption spectrum (Figure 5-4), it was determined that these particles have a size of 5.5 nm. The size has been calculated using an empirical sizing relation dependent on the band gap.[53] The concentration of the nanocrystal solution is $2*10^{-4}$ M. The clear peak in the UV-VIS spectrum indicates a high monodispersity.

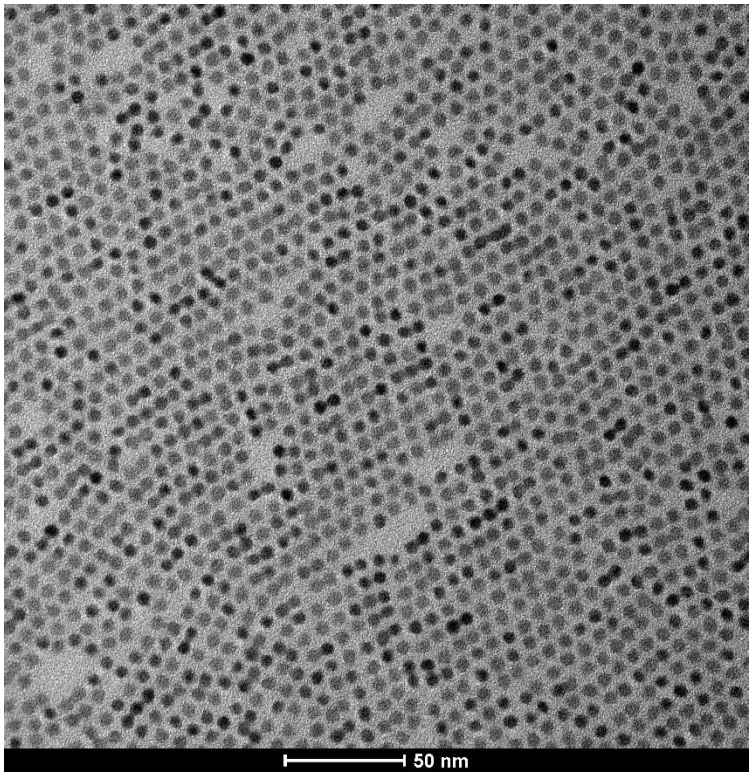

Figure 5-3: Monodisperse spherical PbSe particles synthesised via hot injection by Joep Peters with a diameter of 5.5 nm

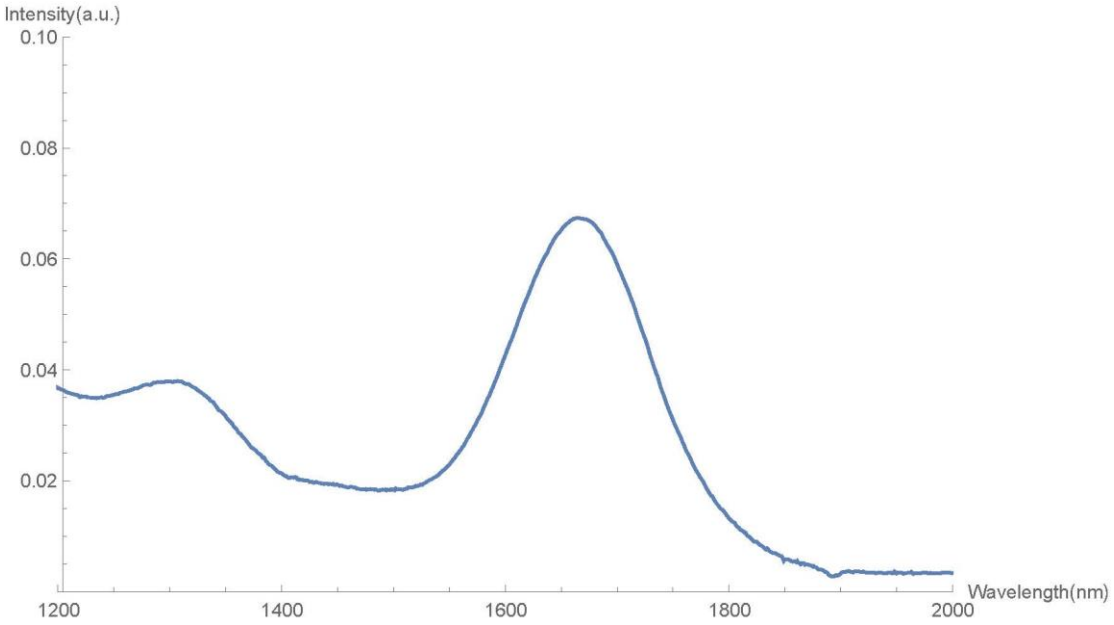

Figure 5-4: UV-VIS spectrum of the PbSe particles shown in Figure 5-3. The two clear peaks visible indicate that the particles have a high monodispersity

5.2. Cation exchange

The goal of the cation exchange is to make CdSe nanocrystals of the same size and morphology as the original PbSe particles. The method for cation exchange is explained in section 4.1.3. After the synthesis, the nanocrystals were characterised using absorption spectroscopy, ICP-OES and Transmission electron microscopy.

The best results were obtained by performing cation exchange on the PbSe nanocrystals shown in Figure 5-3. The colour of the nanocrystals changed from brownish black to orange, which stems from the band gap difference between PbSe and CdSe of the same size.

In figure Figure 5-5 an absorption spectrum of the synthesised CdSe is shown. There is a small peak visible that corresponds to CdSe, but it is not as sharp as for CdSe synthesised via hot injection[54]. This can be a result of the low concentration CdSe used in the measurement or because the CdSe was made out of cation exchange and not by a direct synthesis. However, Groeneveld *et al.*[55] found absorption spectra after cation exchange from ZnSe to CdSe comparable to CdSe synthesised via hot injection. The peak corresponding to PbSe is gone however, indicating that there are no PbSe nanocrystals present anymore.

Using ICP (section 4.2.2) it was determined that the cation exchange was successful and that there was 12 times as much cadmium in the sample than lead, leading to a conversion rate of 92%. This assumes that there is no cadmium oleate left in the sample. Since the nanocrystals are washed twice, there is reason to believe that there is still some cadmium oleate present in the sample and that the actual ratio of CdSe/PbSe is a bit lower.

The concentration nanocrystals was determined to be $1.15*10^{-6}$ M. There was 85 µL of PbSe used for the cation exchange, which corresponds to $1.7*10^{-8}$ mole. Since the cation exchanged

product was dissolved in 2 mL, the maximum yield was $8.5*10^{-6}$ M. The actual yield was thus 13.5%.

Using TEM, it was determined that the nanocrystals have the same size and shape as the PbSe particles and the same crystallinity, since the reflections in the electron diffractogram appear at the same distances for the CdSe when compared to an electron diffractogram of a PbSe square superstructure (Figure 5-6).

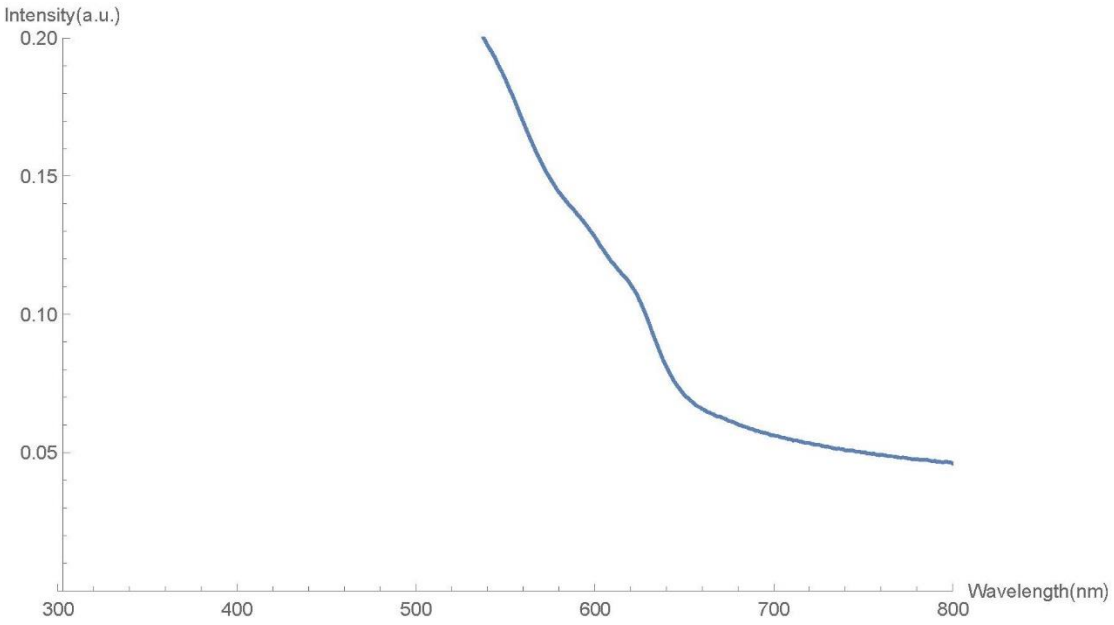

Figure 5-5: UV-VIS absorption spectrum of CdSe. The peak that is expected for CdSe around 600 nm is not sharp, as is expected for CdSe nanocrystals

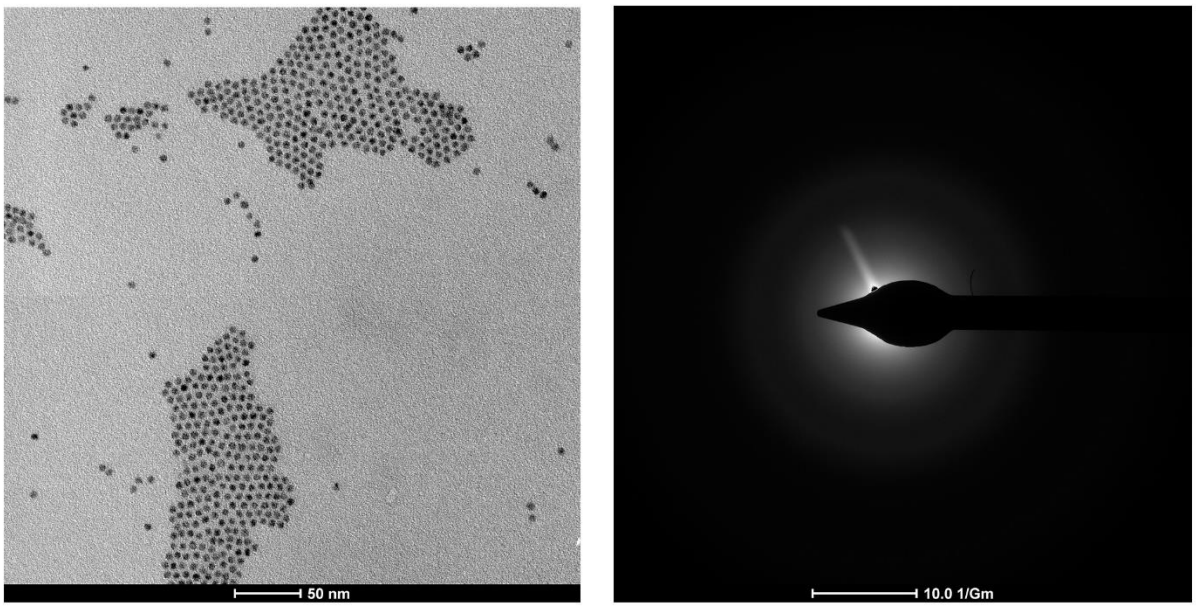

Figure 5-6: a) TEM image of spherical CdSe nanocrystals with a diameter of 5.5 nm made by cation exchange. b) Corresponding electron diffractogram, which has its reflections at the same distances as the electron diffractogram of PbSe.

5.3. Oriented attachment

This section will be split in three parts. First, the effects of various conditions on the oriented attachment results will be explained to give an overview of oriented attachment. Then, the results of the oriented attachment with only PbSe while keeping these conditions in mind will be discussed, including a discussion about the found superstructures. Last, the results of the oriented attachment with CdSe and a mixture of PbSe and CdSe while keeping the reaction conditions in mind will be discussed. This section will end with a recap of all the oriented attachment results and will discuss the insights found in the oriented attachment process.

5.3.1. Reaction conditions

Different reaction conditions have been varied during the oriented attachment experiments. The following conditions will be discussed in this section:

- Nanocrystal size
- Temperature
- External vibrations
- Nanocrystal concentration
- Ethylene glycol
- Reaction time
- Toluene volume
- Added Pb precursor
- Added surfactant

It was found that these factors all can have a different influence on the oriented attachment process and its results. Therefore, it was very important to try to minimise the variations of all the factors, to keep the external variations to a minimum.

Nanocrystal size

The nanocrystal size can be controlled in the hot injection experiment. However, in this thesis, particles made by Joep Peters with a size of 5.5 nm were used. Particles with a size of 5.5 nm are used because smaller particles are more unstable (for example, melting more easily), whereas large particles do not perform oriented attachment.

Nanocrystal concentration

The nanocrystal concentration is important for the success of the oriented attachment process. A too low concentration or bad spreading leads to patches of nanocrystals that are spread over the surface with some oriented attachment. A too high concentration or a bad spreading leads to very messy structures with lots of double layers. A nanocrystal amount of around $1.35*10^{-7}$ mole was most often used in this thesis and was found to give satisfying results (see Figure 5-7). This concentration was achieved by diluting the original nanocrystal solution with a concentration of $2*10^{-4}$ M. Depending on the concentration of nanocrystals, the toluene volume was varied.

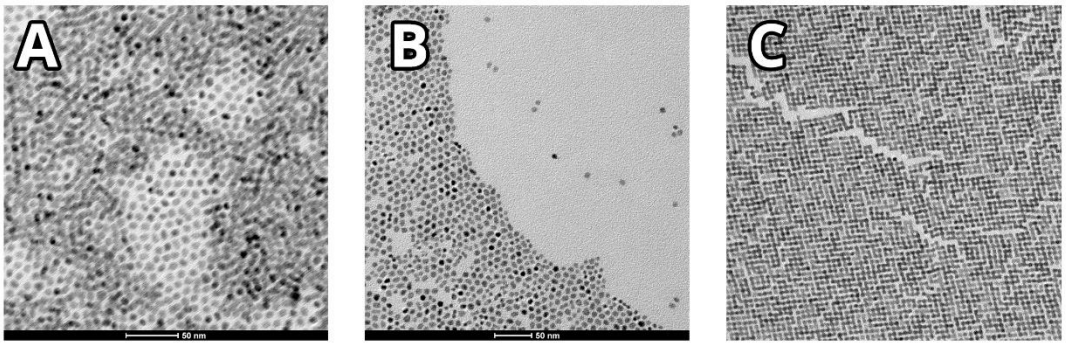

Figure 5-7: a) A high concentration (result of a low spreading) of nanocrystals leads to patches of nanocrystals spread over the substrate. b) A low concentration (result of low spreading) of nanocrystals leads to lots of double layers. c) A concentration of $1.35*10^{-7}$ mole leads to nice ordering over the substrate. Result was achieved in a different experiment.

External vibrations & wind effects

The oriented attachment is carried out in a glovebox and heating is done on a heating plate. The glovebox contains a blower to maintain circulation inside, which generates vibrations and wind. The heating plate also contains a fan to cool itself, which generates a lot of local vibrations and wind. In the oriented attachment results, these effects are visible as broken structures or double layers (see Figure 5-8).

These effects introduce multi-layers in the sample, which are unwanted as a single layer of nanocrystals is desired. Therefore, these effects were if possible eliminated. The vibration effects of the heater could not be eliminated while heating.

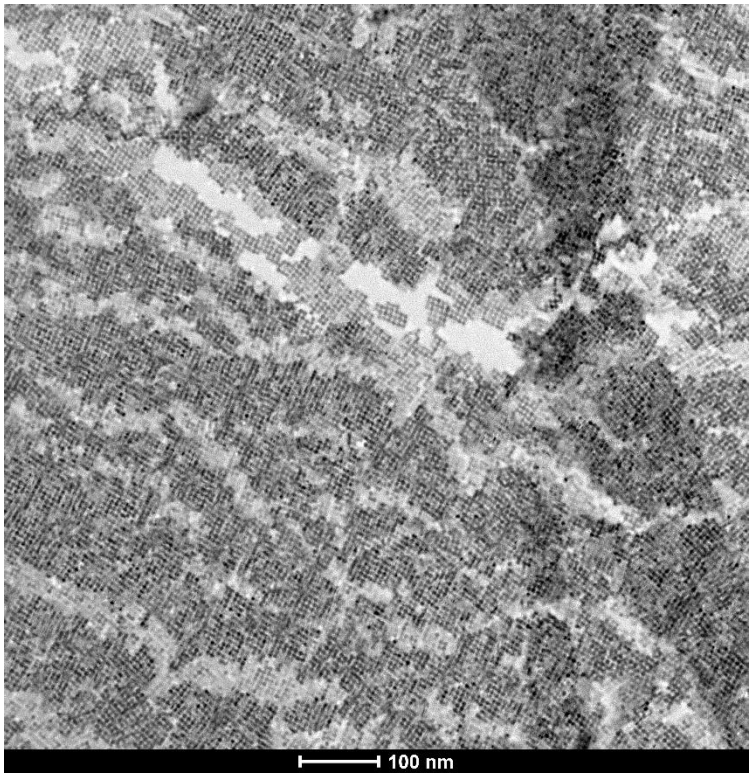

Figure 5-8: Wind and vibration effects cause breaking of the superlattices and multi-layer formation

The wind effects are also very recognisable on a larger scale (see Figure 5-9), showing a wave-like effect of nanocrystals on top of each other. The blower of the glovebox was in later experiments turned off, but attachment results found were unsatisfactory due to oxygen effects. These effects were probably unrelated to the vibration and wind effects, but time constraints did not allow further investigation.

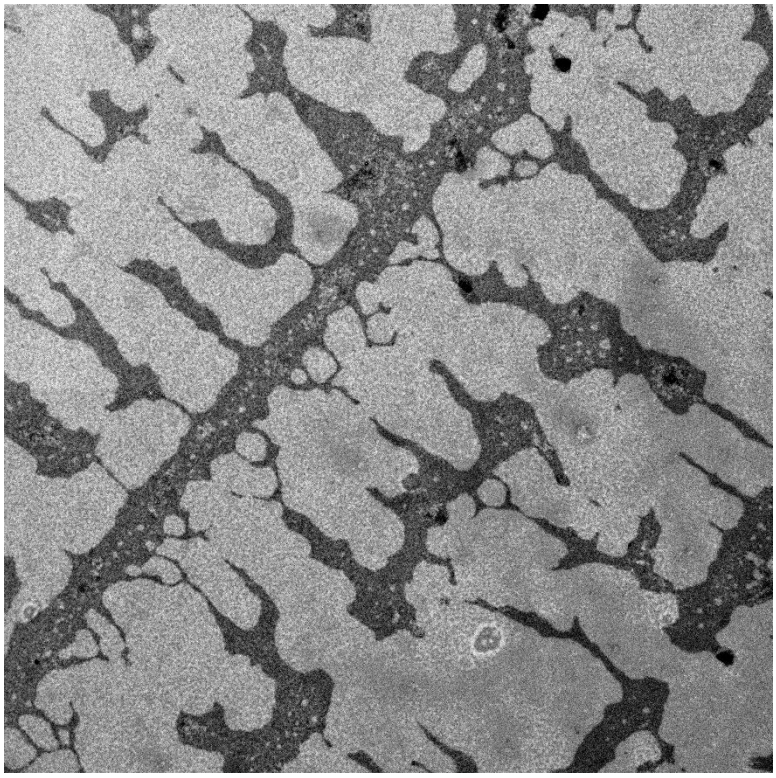

Figure 5-9: Wave-like effects caused by wind in the glovebox

Toluene volume

In this thesis, the toluene volume that was added was varied to see the effect on the oriented attachment results. With a decreasing concentration of nanocrystals, the toluene volume added to the EG surface was proportionally increased to ensure that the same amount of nanocrystals was used in the experiments. The usual oriented attachment experiments are carried out with 350 µL of nanocrystal solution on 6.5 mL of ethylene glycol. In Figure 5-10, it can be seen that this leads to square superstructures. These results were found using a reaction temperature of 22 °C and a reaction time of one hour. Heating was applied to 45 °C for 20 minutes.

It was found that by repeating this experiment, comparable results are produced, leading to the conclusion that this experiment is well reproducible.

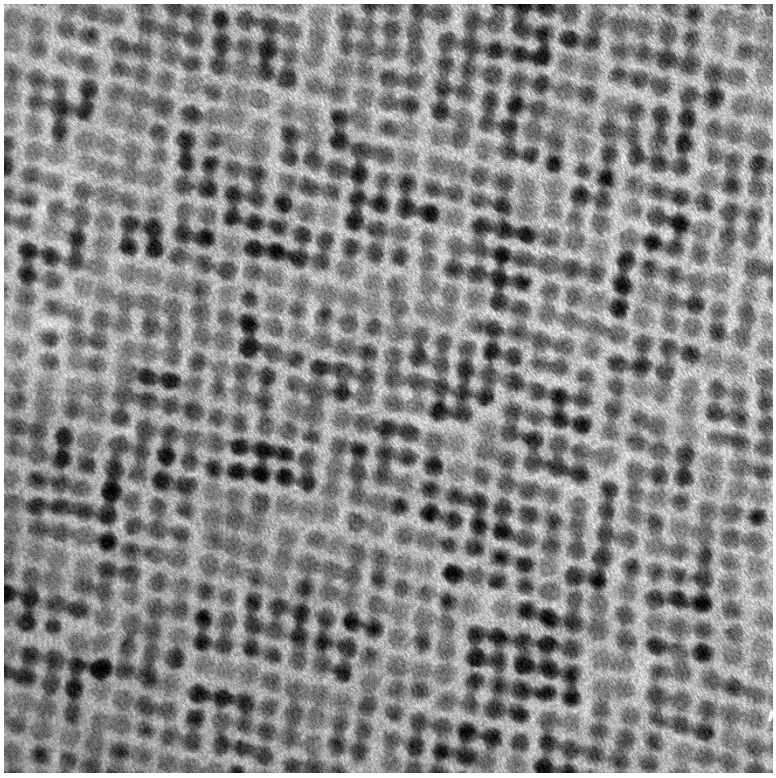

Figure 5-10: Square superstructures made by oriented attachment

When the amount of nanocrystal solution is doubled to 700 µL, other structures such as zigzags and honeycombs were found (Figure 5-11). This is probably a result of the nanocrystals having a greater possibility to stick to the toluene-air interface, with their {111} facets, which aligns them to a honeycomb structure with the substrate perpendicular to the {111} facets.[5,6] With less toluene, the nanocrystals will stick to the toluene-ethylene glycol interface. They attach to this interface with their {110} facets, forming square structures.[5] Other toluene amounts have been tried as well, but these did not deliver satisfactory results, because of insufficient evaporation or oxygen effects.

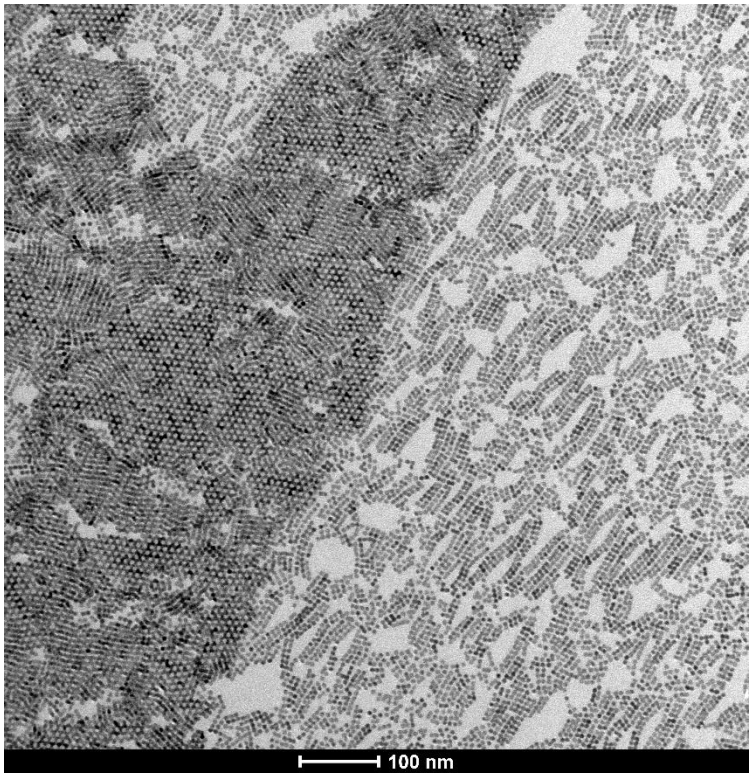

Figure 5-11: Honeycomb and zigzag structures made by oriented attachment

Temperature

During the oriented attachment process the temperature can be controlled via a heating plate. The heating provided was only directly on the plate, the temperature of the glovebox could not be controlled and varied depending on the temperature in the glovebox room, which was not controlled.

The temperature was varied during the oriented attachment process or directly after the process. In the second variation, a webcam was used to check the toluene volume (by checking the reflections on the surface). After all toluene had evaporated, the system was left for another half an hour, after which the temperature variation was applied. An advantage of this approach is that the heating plate is left off during the attachment, eliminating vibrations coming from the fan. When temperature variations are applied during the attachment with the heating plate, the plate creates vibrations, influencing the attachment process.

It was found that when a little heating (30 °C) is applied during the oriented attachment process, the process is sped up, since the toluene evaporated faster. This meant that if there was 700 µL of nanocrystal solution used in the reaction, it lead to ordered square superstructures together with some lines and zigzag-like structures, instead of a mixture of honeycombs, lines and zigzag-like superstructures (see Figure 5-12). means that it is more likely that square structures are found.

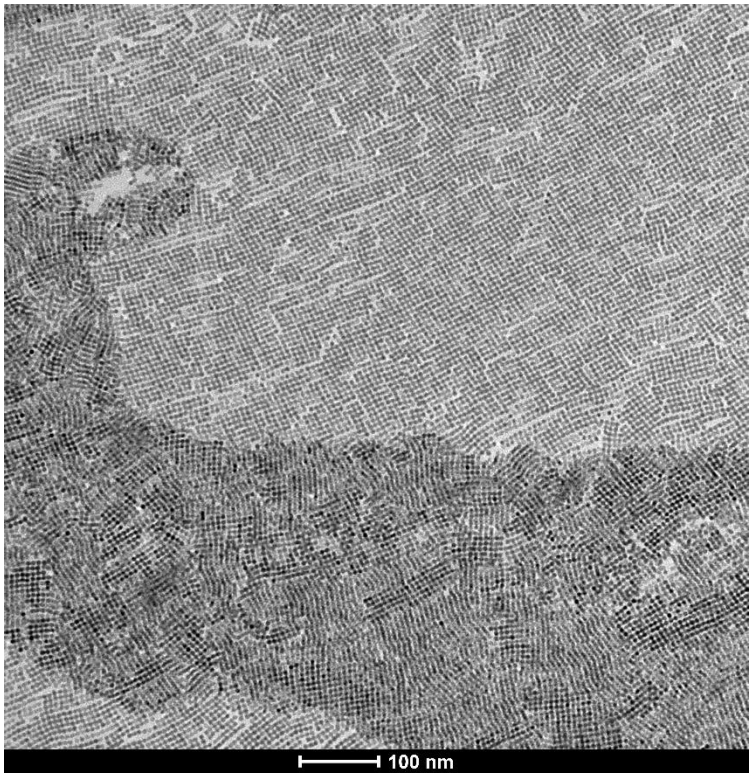

Figure 5-12: Square superstructures with some linear and zigzag-like structures, achieved by oriented attachment using 700 µL of nanocrystal solution and a reaction temperature of 30 °C

When heating was applied after the oriented attachment process (45 °C), it was found that the necks between nanocrystals were a little more molten together, resulting in better superstructures. When the heating was turned up to 65 °C, the resulting superstructures were molten as in Figure 5-13. This leads to the conclusion that there is an optimum in the heating temperature. If the temperature is higher, it degrades the superstructures.

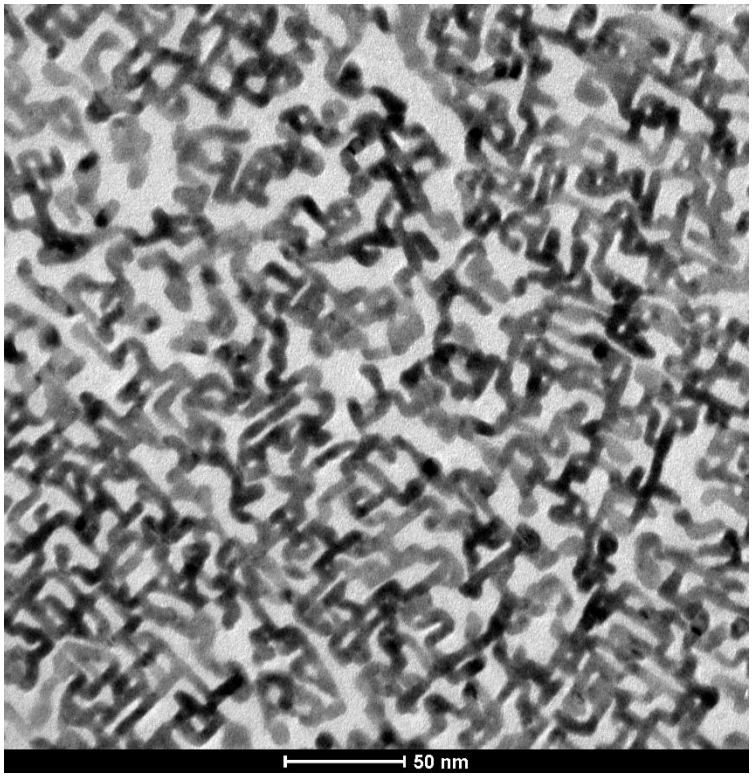

Figure 5-13: Molten superstructures after heating to 65 °C after the oriented attachment reaction

Ethylene glycol

The oriented attachment experiments are carried out on an ethylene glycol substrate. The quality of the ethylene glycol influences the oriented attachment results. 6.5 mL of ethylene glycol is put in a petri dish with a diameter of 29 mm. This is not varied for the experiments, except the experiments where 1.05 mL of nanocrystal solution was added. 6 mL of ethylene glycol was used there, to prevent the petri dish from overflowing.

It was found that the quality of the oriented attachment results depends on the quality of the ehtylene glycol. The ethylene glycol is degassed before it is introduced in the glovebox. When this is not done carefully, it is found that the results are molten (see Figure 5-14), leading to the suspicion that there is oxygen in the ethylene glycol which effects the oriented attachment process, leading to oxidation of the structures.

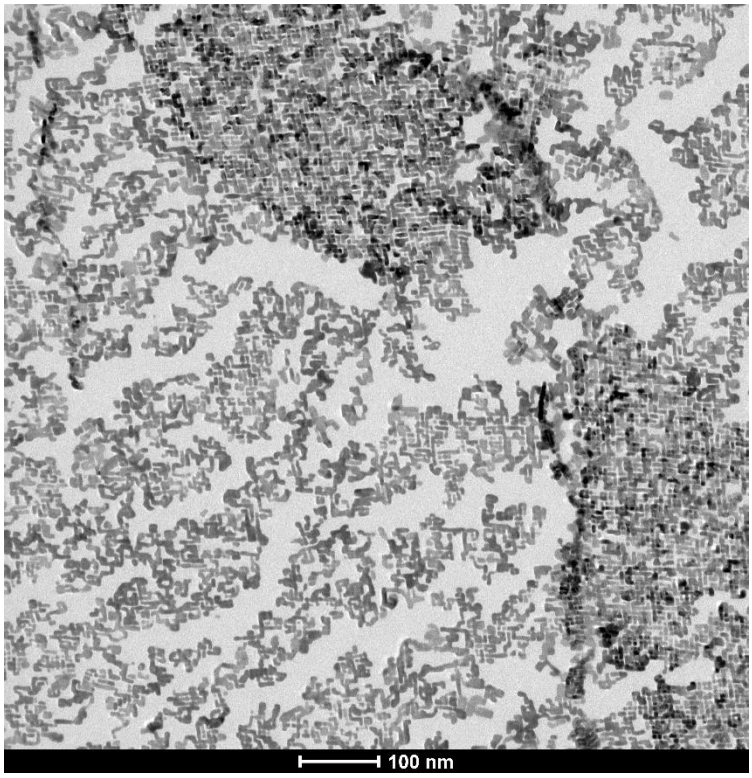

Figure 5-14: Oriented attachment of square superstructures. The structures are molten because of oxygen in the ethylene glycol

Reaction time

A webcam was used to check the toluene volume in the oriented attachment process. The reaction time was based on this. After all the toluene had evaporated, the reaction was left for 30 more minutes. It was found that for most reaction conditions, a reaction time of 1 hour was sufficient. When the blower is turned off and there are 8 petridishes with at least 700 µL of nanocrystal solution, it was found that a reaction time of 1 hour is not sufficient to let all the toluene evaporate (Figure 5-15). The heating afterwards to 45 °C leads to a too fast evaporation of toluene, leading to unattached structures. A reaction time of around 3 hours was needed in this case to let the toluene evaporate, leading to square superstructures.

After the reaction has finished, heating was applied, which was done for 20-30 minutes, regardless of other reaction conditions, to smoothen the surface of the superstructures.

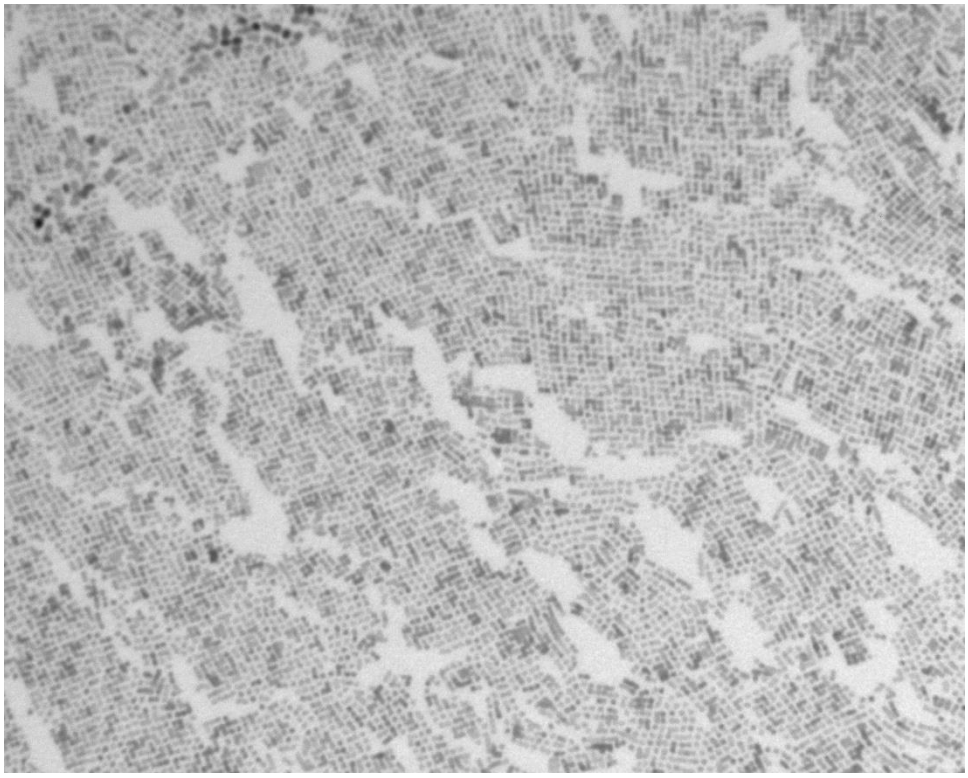

Figure 5-15: Unattached dots, because heating was applied too early

Added Pb precursor

During the course of this thesis it was noted that by adding lead oleate to the nanocrystal solution, the resulting superstructures consisted of larger fields instead of smaller patches and double layers that are sometimes found (Figure 5-10). This is done by adding an amount of lead oleate that corresponds to a concentration that is 200 times as high as the concentration of nanocrystals in the solution. This means that in the case of a nanocrystal concentration of $1.35*10^{-7}$ mole on the surface, there was $2.7*10^{-5}$ mole of lead oleate.

The reason that lead oleate improves the oriented attachment process is attributed to it helping forming the necks between the nanocrystals, via an ion-by-ion process (see section 3.4.4.

Added surfactant

Oleic acid has been added directly to the ethylene glycol because it has the capabilities of destabilizing the surface by lowering the surface tension, leading to a better wetting, which makes the oriented attachment more spread out. This has been shown for a concentration of $2.7*10^{-5}$ mole (Figure 5-16).

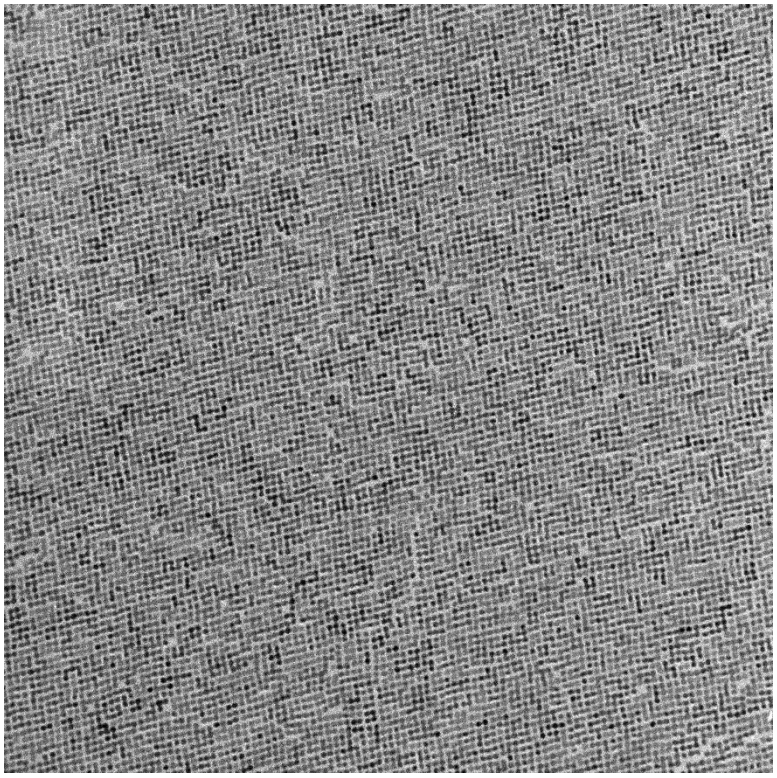

Figure 5-16: Spread out nanocrystals performing oriented attachment, because oleic acid destabilised the ethylene glycol surface

Without oleic acid, there is still oriented attachment happening, however, the structures consist of smaller patches (see Figure 5-17). Note that this experiment was done using the same condition

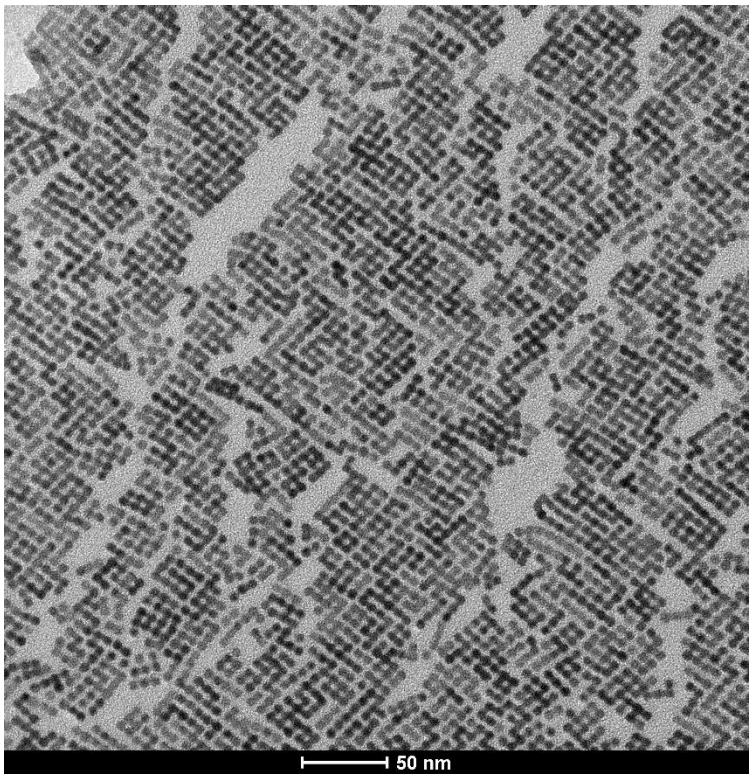

Figure 5-17: Without using oleic acid to destabilise the surface, smaller patches of PbSe superstructures are formed

When the concentration was halved, the same phenomenon was observed, although it seemed that the amount of honeycombs was increased (Figure 5-18). It was also found that using too much oleic acid stops the attachment process, leaving only assembled nanocrystals.

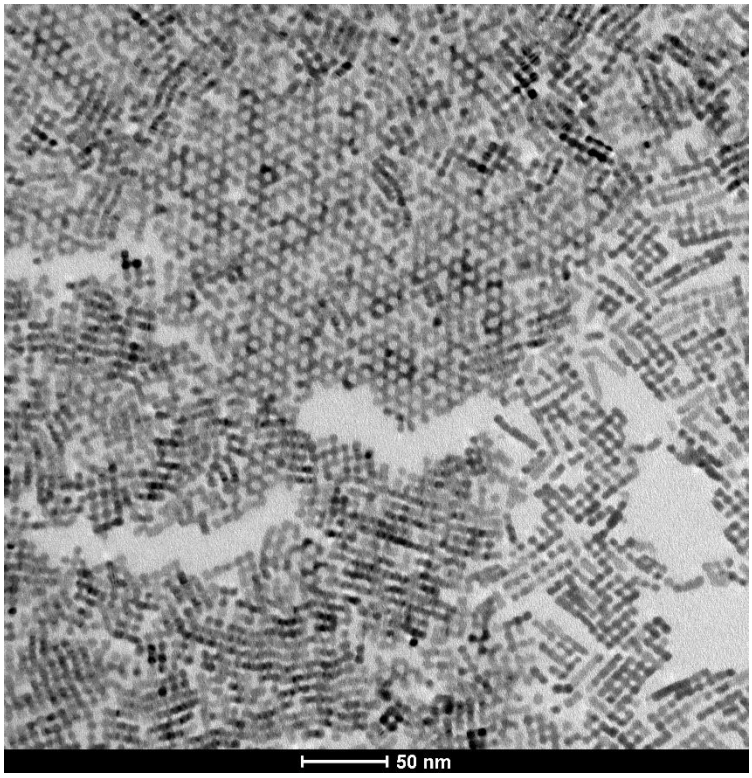

Figure 5-18: The amount of honeycombs seems to increase when less oleic acid is used

5.3.2. PbSe oriented attachment results

A large variety of oriented attachment experiments with PbSe were done to make square superstructures and to go from there to oriented attachment with PbSe and CdSe. In this chapter, the results of the oriented attachment experiments with only PbSe will be shown and discussed. It was found that PbSe can perform oriented attachment and form different kind of structures, depending on the reaction conditions. The square and honeycomb structures are shown to have atomical alignment using electron diffraction.

As said, the goal of the oriented attachment experiments was to successfully synthesise square superstructures of PbSe nanocrystals. This was done successfully. It was found that the best attachment results were found using a nanocrystal volume of 350 µL, consisting of PbSe nanocrystals, Pb oleate and toluene. This was added to a petri dish filled with 6.5 mL ethylene glycol, on which $2.7*10^{-5}$ mole of oleic acid was added to the surface. Heating was not applied during the oriented attachment process which took 1 hour. After 1 hour, heating was applied for 20-30 minutes.

Using these conditions and in multiple experiments, square superstructures of large sizes were found (see Figure 5-19).

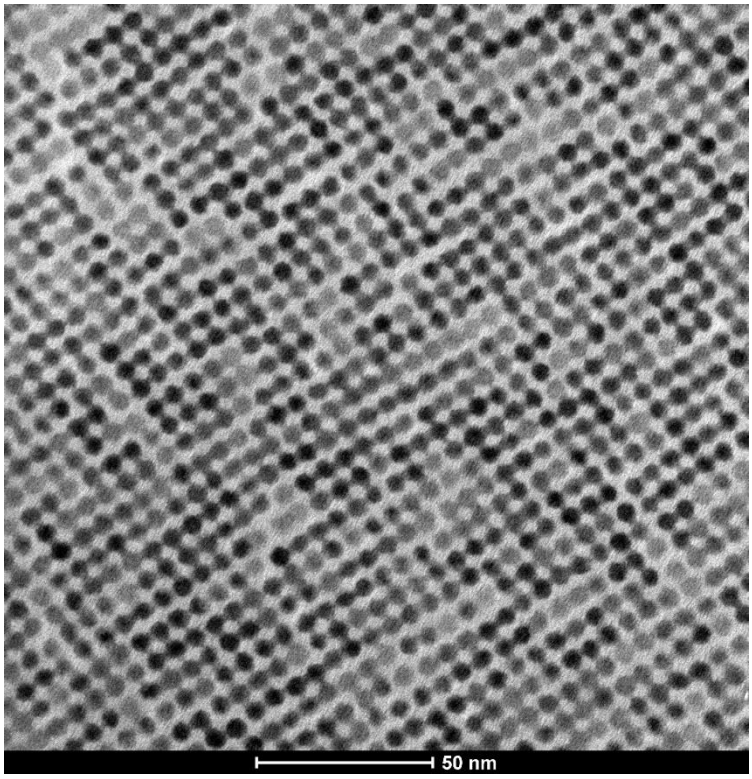

Figure 5-19: TEM picture of square superstructures

There is a clearly observable order in the superstructure. This is also shown in the electron diffractogram, which is shown in Figure 5-20. In this electron diffractogram, it can be seen that the square structure found has atomical order that it has four-fold symmetry. It is not possible to determine if the superstructure is a single crystal directly from this electron diffractogram. To do this, the Debye-Scherrer formula should be used[56], which hasn't been done.

The found electron diffractogram spots correspond to the facets that are parallel to the electron beam. The facet of the nanocrystals that these spots correspond to can be calculated

(see appendix B). From these calculations, the conclusion can be made that the {100} and {110} facets are standing perpendicular to the substrate, which can only be the case of the <001> axes of the single nanocrystals are perpendicular with respect to the substrate.

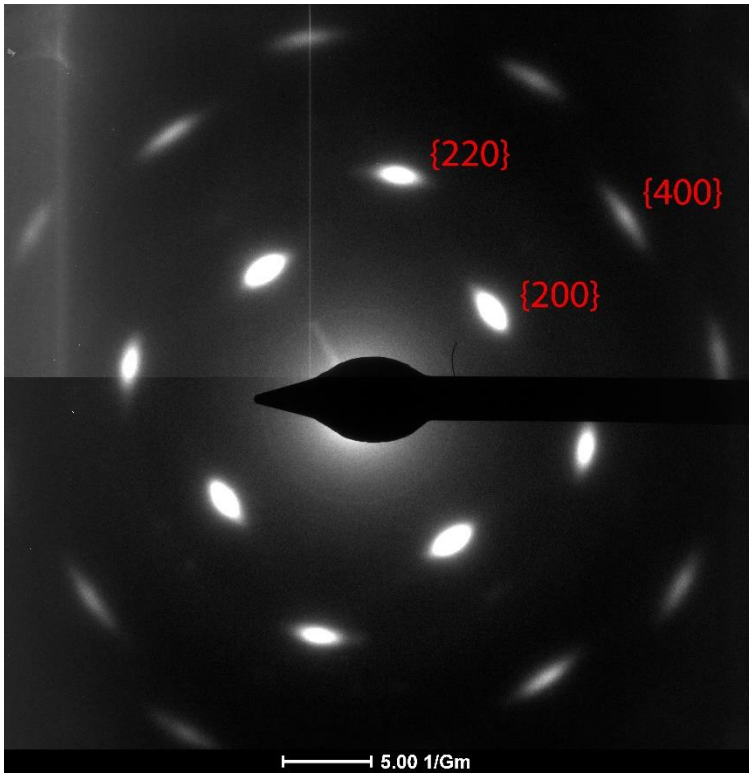

Figure 5-20: Electron diffractogram of the square superstructure shown above with the corresponding facets indicated

Square superstructures were also found when the toluene volume was doubled to 700 µL and heating to 30 °C was applied during the oriented attachment process, which took again 1 hour. Heating to 45 °C was also applied after the process for 20-30 minutes. All the other factors were kept the same as the earlier described experiment. It was found that the superstructures were not as good as in the experiment with only 350 µL of nanocrystal volume. These results are shown in Figure 5-21.

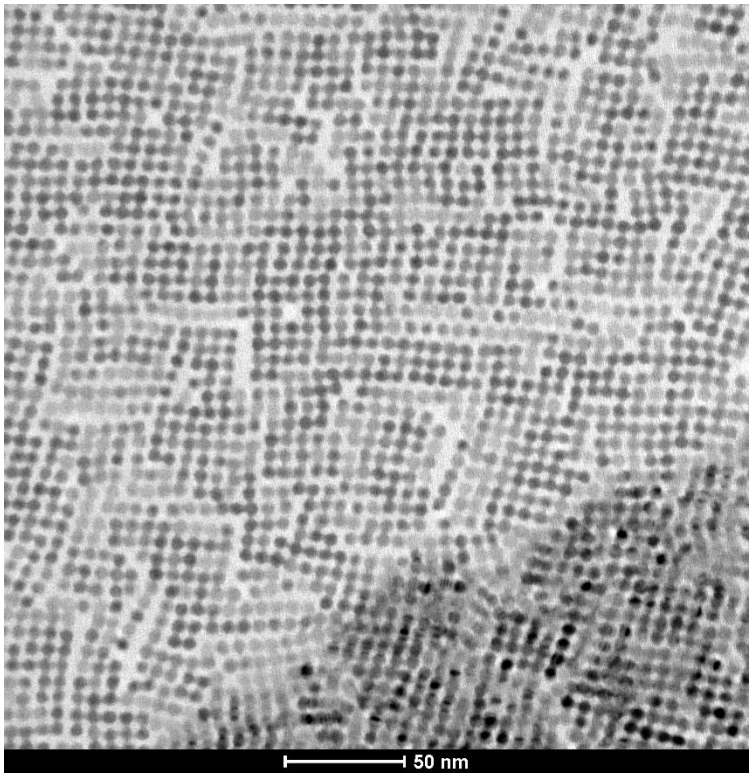

Figure 5-21: Square superstructures obtained after heating during the oriented attachment process

During the course of this master's thesis, honeycomb structures were synthesised as well. Honeycomb superstructures are very interesting because of their structural and electronical similarities to graphene. It is however still not possible to synthesise them reproducibly. Therefore, some work of this master's thesis has been done on the honeycomb superstructures.

The honeycombs found during this thesis were synthesized by dropcasting a nanocrystal solution of 700 µL, which consists of around $1.35*10^{-7}$ mole PbSe nanocrystals, Pb oleate and toluene on 6.5 mL of ethylene glycol in a petri dish. There was $2.7*10^{-5}$ mole or $1.35*10^{-5}$ mole oleic acid added to the surface. The honeycombs that were found were always found between other structures such as linear and zigzag structures, which were more abundant (Figure 5-22).

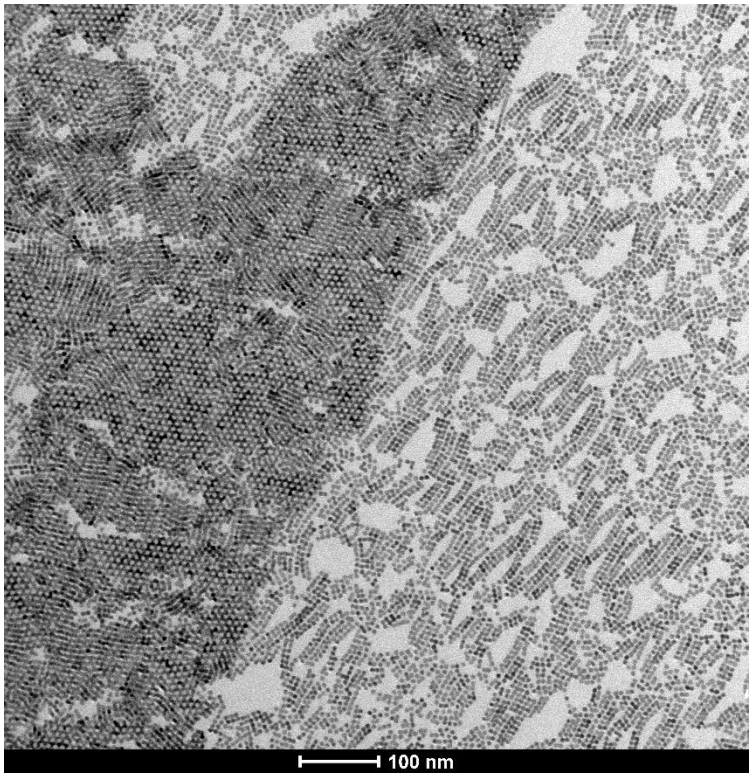

Figure 5-22: Honeycomb structures found during this thesis, accompanied by linear and zig-zag structures

Using the described method, it was possible to synthesise honeycomb superstructures in multiple experiments using the same variations (see for example Figure 5-23), showing the reproducibility of the method. Joep Peters and Carlo van Overbeek have also reported success using this method.

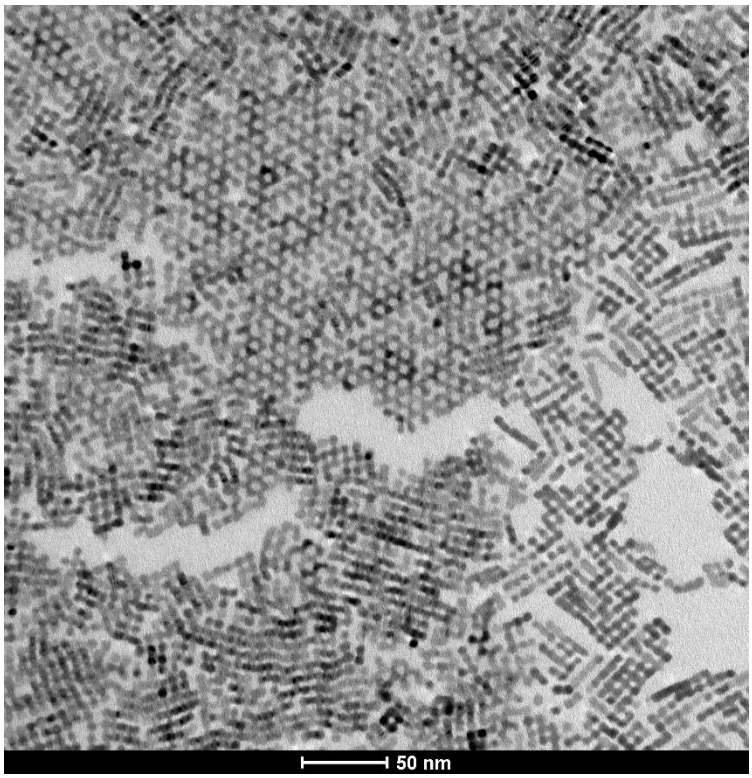

Figure 5-23: Honeycomb superstructures synthesised in another experiment, again accompanied by other structures

It is not possible yet to synthesis large honeycomb superstructures, the largest superstructure found is shown in Figure 5-24 together with the corresponding electron diffractogram. It has been tried to get larger superstructures, by using an even larger amount of nanocrystal solution, but these experiments were unsuccesfull, because there were oxygen and time constraint factors that influenced the oriented attachment process.

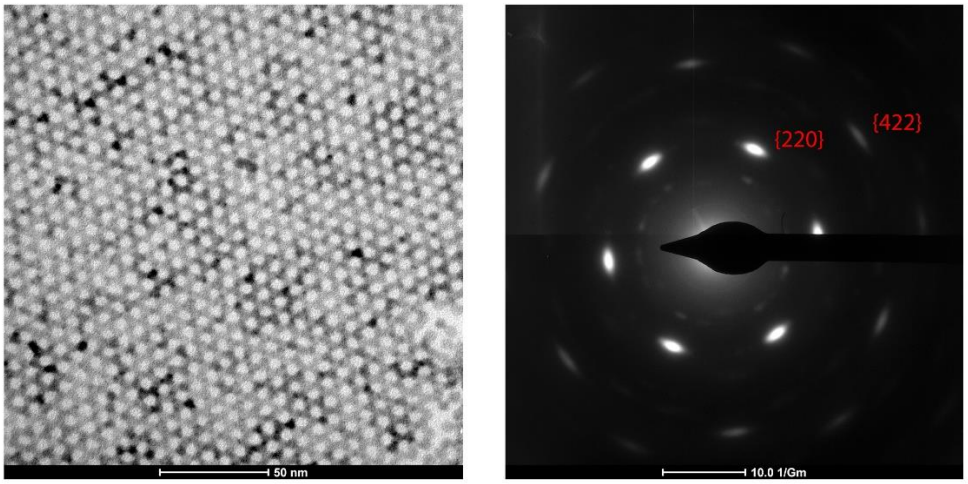

Figure 5-24: Honeycomb patch with its corresponding electron diffractogram with the corresponding facets indicated

In the honeycomb electron diffractogram, it can be easily seen that the nanocrystals have atomical order and have six-fold symmetry. The electron diffractogram spots correspond to the facets that are parallel to the electron beam. The facet of the nanocrystals that these spots correspond to can be calculated (see appendix B). From these calculations, the conclusion can be made that the {110} facets are standing perpendicular to the substrate, which can only be the case if the <111> axes of the single nanocrystals are perpendicular with respect to the substrate.

A superstructure that is often (if not always) found together with and in close proximity to honeycomb superstructures is the zigzag superstructure (see Figure 5-25).

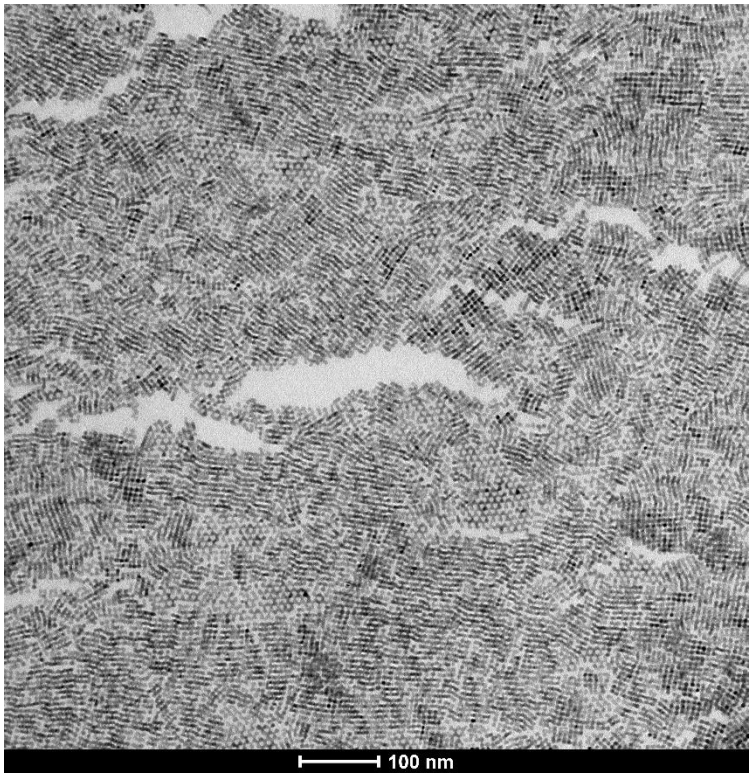

Figure 5-25: Zigzag structures are often found together with honeycomb structures

Because this structure is most often found together with the honeycomb superstructure, it is likely that there is a relationship between the two. Although the exact relationship is not yet known, it is possible to speculate. The zigzag structure is, as can be seen, a densely packed superstructure (more dense than the honeycomb structure), consisting of parallel waved wires. This makes it possible that the formation of honeycombs and zigzags with respect to each other is dependent on the local concentration or the interfacial tension between the nanocrystals and the glovebox atmosphere. If this is the case, zigzags might be formed when honeycomb-like structures are assembled and then subsequently are squashed together, leading to the higher packing. It does not however explain why there are also zigzag-like structures found when there are nog honeycomb structures, but only square and linear structures.

Linear superstructures have been found together with honeycomb and zigzag superstructures. They were also found together with squares, but were often less pronounced in that case.

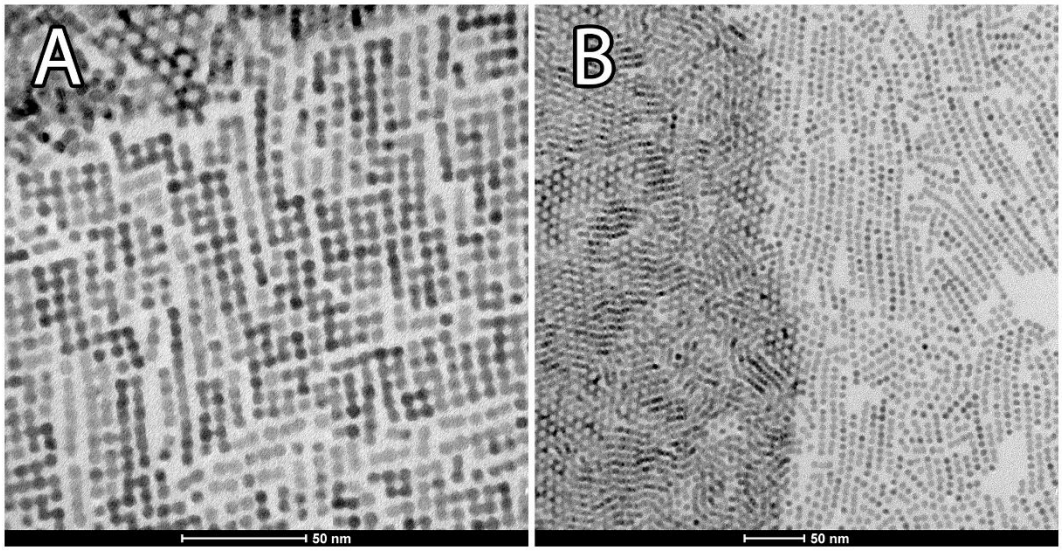

Figure 5-26: a) Linear structures together with square structures. b) Linear structures together with zigzag and honeycomb structures.

What is remarkable about linear structures is that they almost always propagate in only one direction and that they can be quite long. This leads to the conclusion that the attachment only happens on one specific facet. The reason for this is not yet known, more research has to be done on this point. However, it is speculated that forces like dipolar interactions might play a role.

5.3.3. PbSe/CdSe oriented attachment results

It has been shown that PbSe alone does perform oriented attachment. However, for reasons that are still unknown, CdSe will not perform oriented attachment. Therefore, oriented attachment experiments with CdSe have been done. Oriented attachment experiments with mixtures of PbSe and CdSe have been done to see what happens with the CdSe dots and to get more insight in the oriented attachment process. There are multiple possibilities, the CdSe dots might get incorporated in a square lattice formed by PbSe. They might also be left out in an early stage, giving PbSe square lattices and loose CdSe dots or patches. It is also possible that CdSe will be incorporated in the self-assembly of a square superlattice, but will be left out when the oriented attachment takes place, leading to defects in the resulting superlattice.

It is hard to synthesise CdSe nanocrystals with the same size, shape and morphology as PbSe nanocrystals via hot injection. CdSe particles obtained by cation exchange performed on the PbSe particles have therefore been used, because then they are ensured to have the same size, shape and morphology as the used PbSe particles. This has also been checked after the cation exchange.

First, an oriented attachment experiment with CdSe alone was done. An estimation of the concentration had to be made, since the absorption spectroscopy results could not be used and the ICP experiments had not yet been done. It turned out that the concentration was far lower than for the PbSe oriented attachment experiments described in section 5.3.2.

An oriented attachment experiment with PbSe alone has been done as a reference. The experiment was done using using a nanocrystal volume of 350 µL, consisting of PbSe nanocrystals, Pb oleate and toluene. This was added to a petri dish filled with 6.5 mL ethylene glycol, on which $2.7*10^{-5}$ mole of oleic acid was added to the surface. Heating was not applied during the oriented attachment process which took 1 hour. After 1 hour, heating was applied for 20-30 minutes. The TEM picture is seen in Figure 5-27. It can be seen that there are superstructures, however, they are molten because there were oxygen traces in the ethylene glycol because of insufficient degassing. This is not a problem for these experiments, because attachment still took place and it was still possible to do an atom-specific analysis.

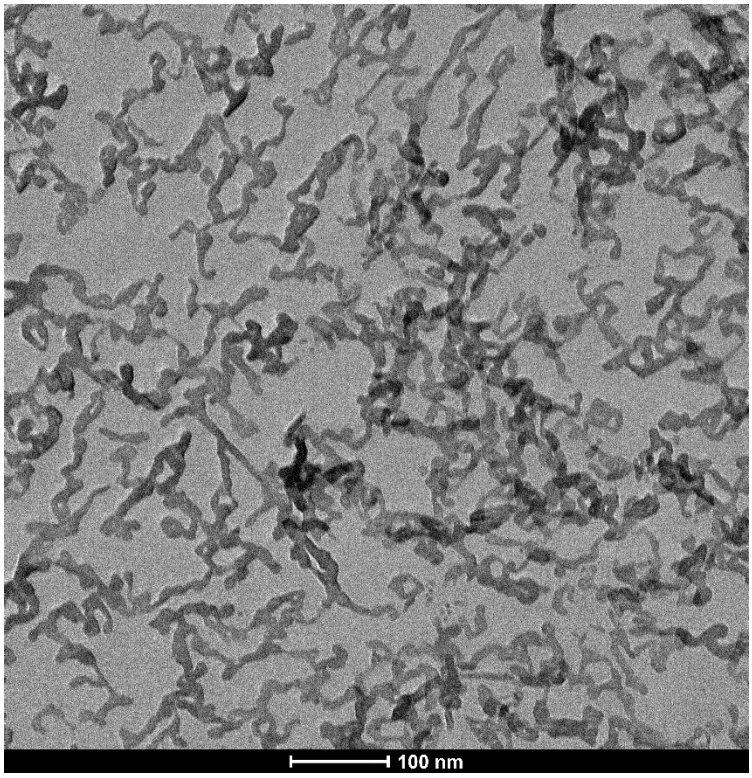

Figure 5-27: Reference PbSe oriented attachment. It can be seen that, although molten, oriented attachment in square-like structures took place

In Figure 5-28 the corresponding EDX spectrum is shown with the corresponding elements already labeled. The carbon and copper peaks in the spectrum correspond to the TEM grid. Using this data, it has been calculated that the atomical concentration of Pb was 51.32% and the atomical concentration of Se was 48.67%. The ratio is not exactly 1:1, because Pb oleate was used in this experiment.

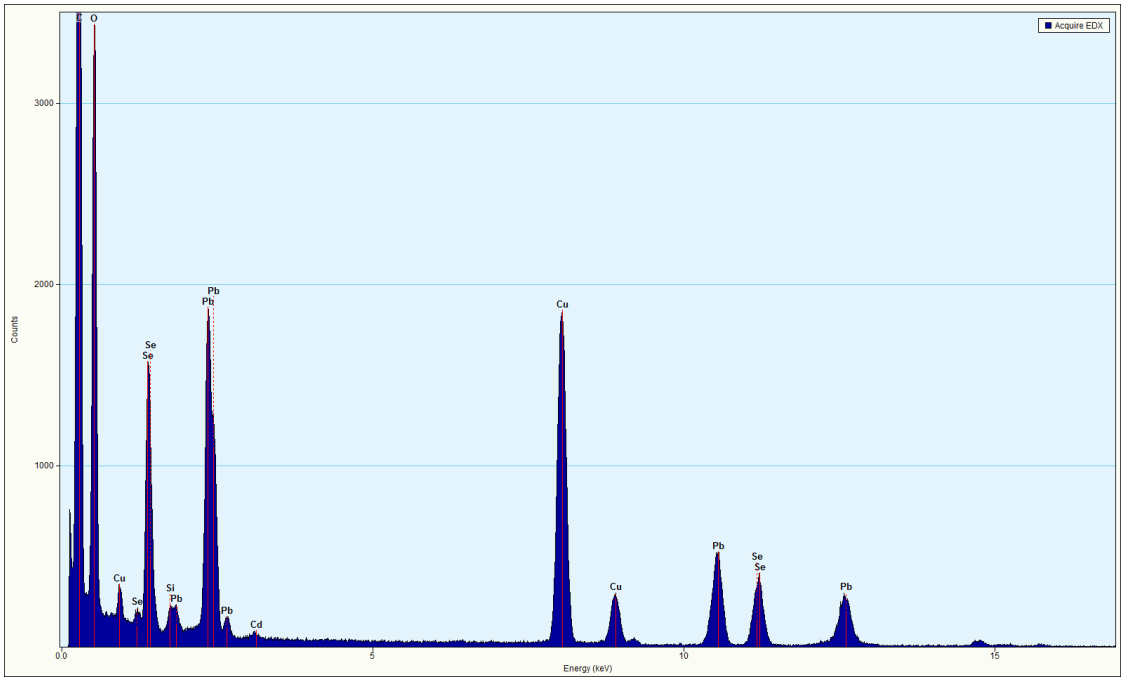

Figure 5-28: EDX spectrum corresponding to Figure 5-27, showing the elements present in the sample. Using this data, it was possible to determine the Pb:Se ratio

For the oriented attachment experiment with only CdSe, 350 µL of a nanocrystal solution consisting of CdSe nanocrystals, the same amount of Pb Oleate as for the PbSe oriented attachment experiments and toluene was dropcasted on a petri dish with 6.5 mL of ethylene glycol. On this ethylene glycol, 2.7*10-5 mole of oleic acid was dropcasted. Heating was not applied during the oriented attachment process which took 1 hour. After 1 hour, heating was applied for 20-30 minutes.

The results can be seen in Figure 5-29. Here, it is clear that, although there is self-assembly (the nanocrystals are ordered very nicely), there is no attachment, the nanocrystals are not connected.

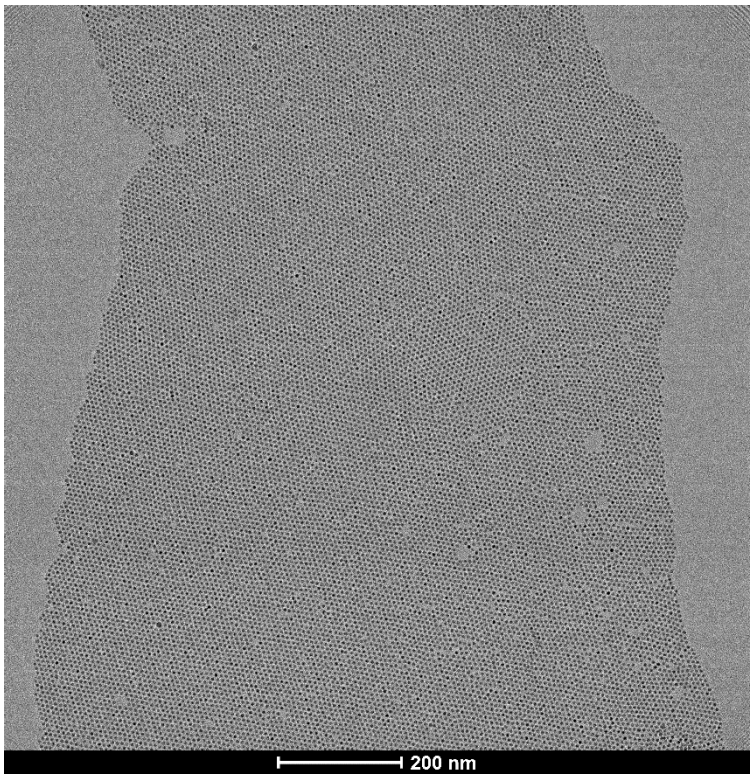

Figure 5-29: CdSe attachment results. There is self-assembly, but no attachment

In Figure 5-30 it can be seen that CdSe will also form double layers (or even more layers) and that these layers contain some ordening as well.

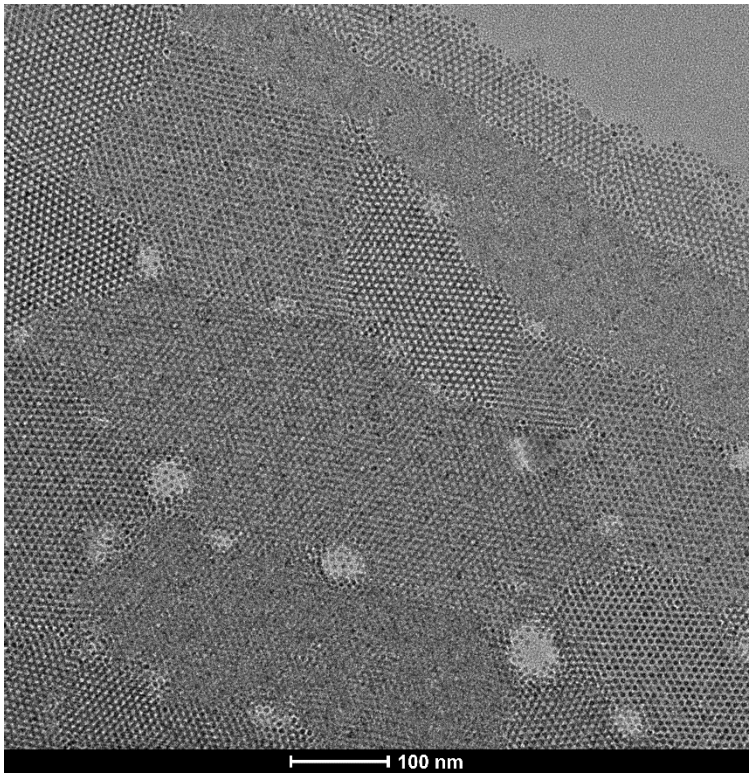

Figure 5-30: Ordering and self-assembly of CdSe multilayers without oriented attachment

Using energy-dispersive X-ray spectroscopy it was possible to determine the amount of Cd, Pb and Se in the region where a TEM picture was made. The EDX spectrum corresponding to Figure 5-30 is shown in Figure 5-31 with the corresponding elements labeled. Using this data, it was calculated that the sample contained 34.19% Se, 58.93% Cd and 6.87% Pb. The measured Cd is probably a bit high, or there is a lot of Cd oleate still present in the sample. However, it shows that there is a very low amount of Pb in the sample, which is probably mostly Pb oleate, showing again that the cation exchange was successful. As discussed in section 5.2, the concentration was $1.15*10^{-6}$ M, of which a part could be Cd oleate.

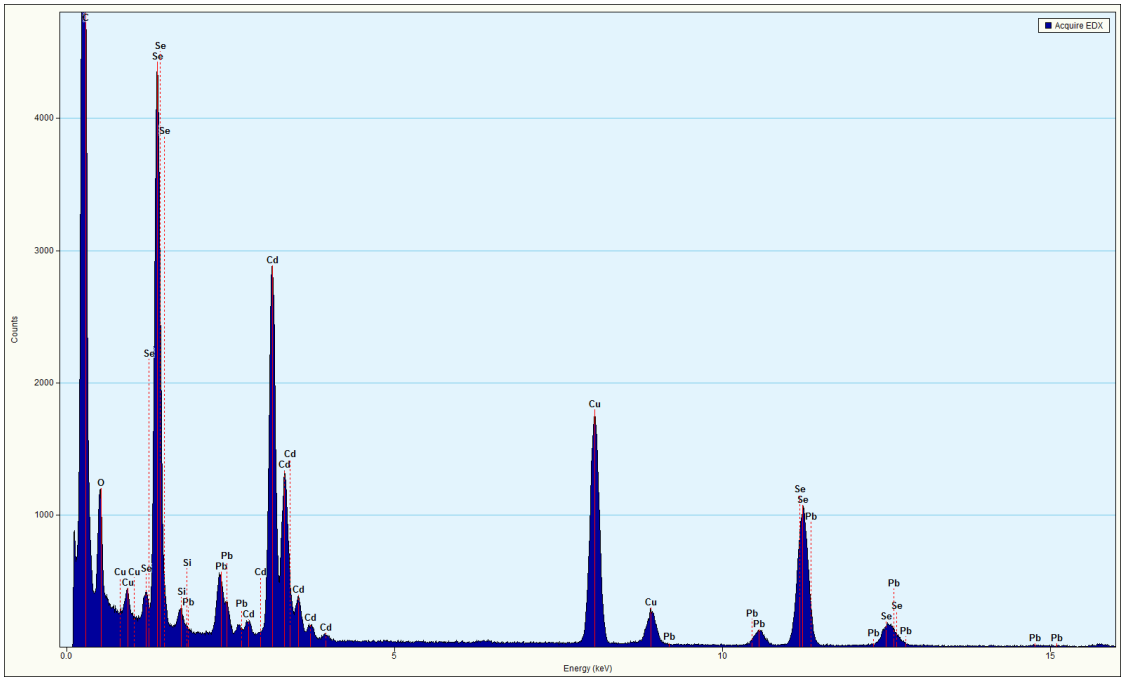

Figure 5-31: EDX spectrum corresponding to Figure 5-30, showing the elements present in the sample. Using this data, it was possible to determine the Cd:Pb:Se ratio

Next, an experiment with a mixture of PbSe and CdSe has been done. Again, 350 µL of a nanocrystal solution consisting of CdSe nanocrystals, the same amount of Pb Oleate as for the PbSe oriented attachment experiments and toluene was dropcasted on a petri dish with 6.5 mL of ethylene glycol. On this ethylene glycol, 2.7*10-5 mole of oleic acid was dropcasted. Heating was not applied during the oriented attachment process which took 1 hour. After 1 hour, heating was applied for 20-30 minutes.

In Figure 5-32 a TEM picture is shown. It can be seen that there are again molten superstructures. However, it can be seen that there are loose dots lying close to the superstructures. There are no dots however between the superstructures. It is of interest to see if the superstructures and the loose dots consist of PbSe or CdSe, or a mixture.

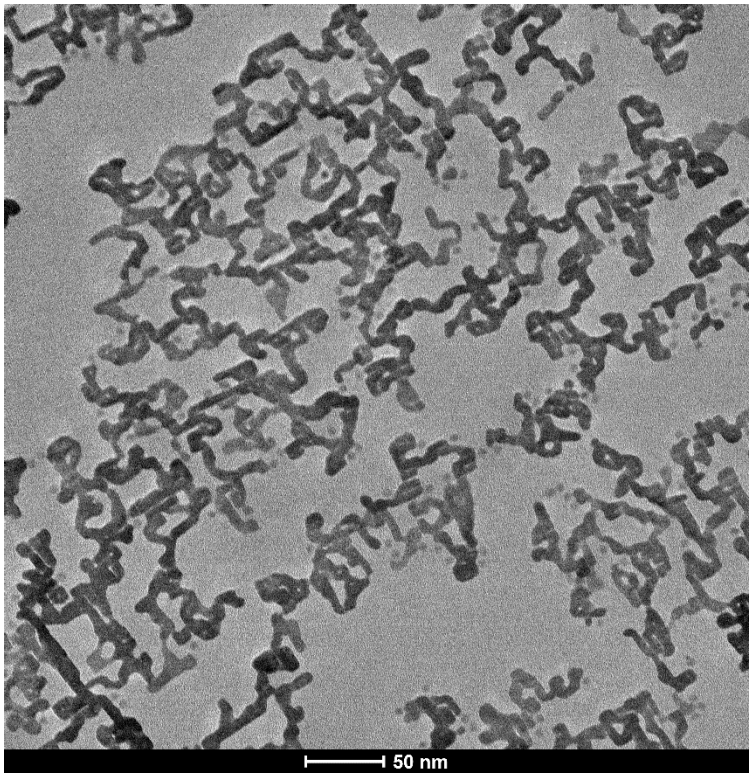

Figure 5-32: Oriented attachment with a mixture of PbSe and CdSe. It can be seen that there are single dots lying between the superstructures

Before atom-specific resolution TEM has been done, an EDX spectrum has been made, which is shown in Figure 5-33. Using this spectrum, it has been calculated that there is 48.04% Se, 49,55% Pb and 2.39% Cd in the sample, which means that there is a very low concentration of Cd, lower than assumed during the synthesis.

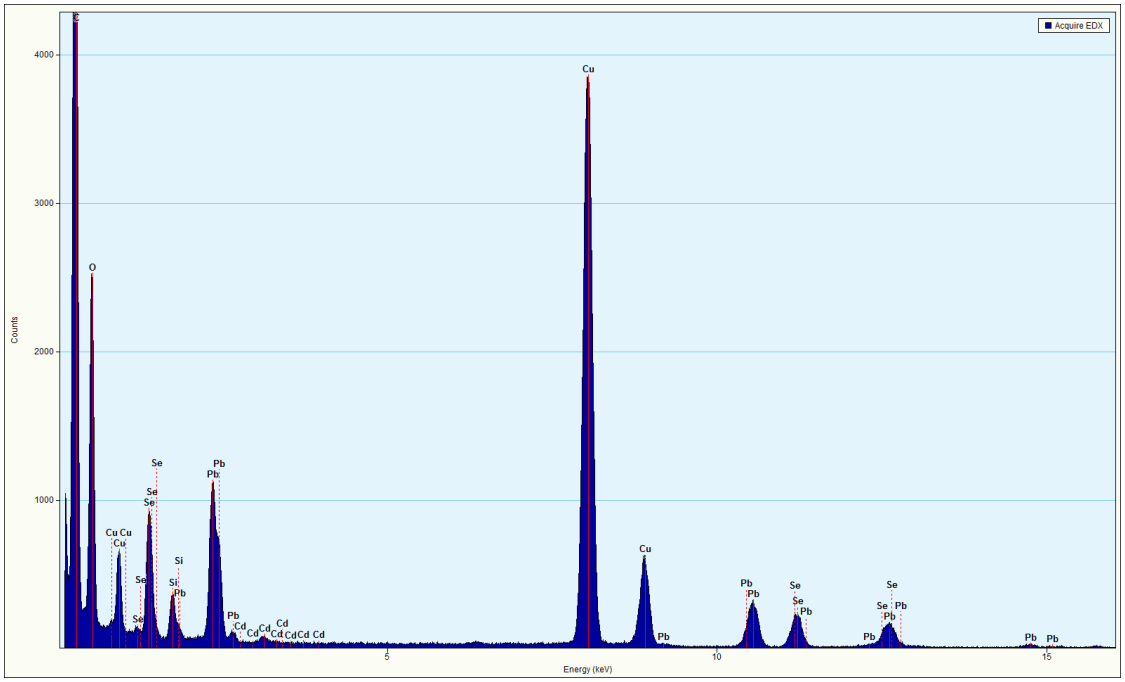

Figure 5-33: EDX spectrum corresponding to Figure 5-32. Using this data, it was possible to determine the Cd:Pb:Se ratio

Using HAADF-STEM combined with EDX, it is possible to use TEM to see the composition of single dots. The resulting HAADF-STEM picture and the atom-specific analysis is shown in Figure 5-34. In the HAADF-STEM picture, the difference between the superstructures and the single dots is clearly visible. In the atom-specific analysis, it can be seen that those single dots mostly consist of Cd and Se, whereas the superstructures are made of Pb and Se, proving that the single dots are made of CdSe and the superstructures of PbSe and that the CdSe is not incorporated in the superstructures.

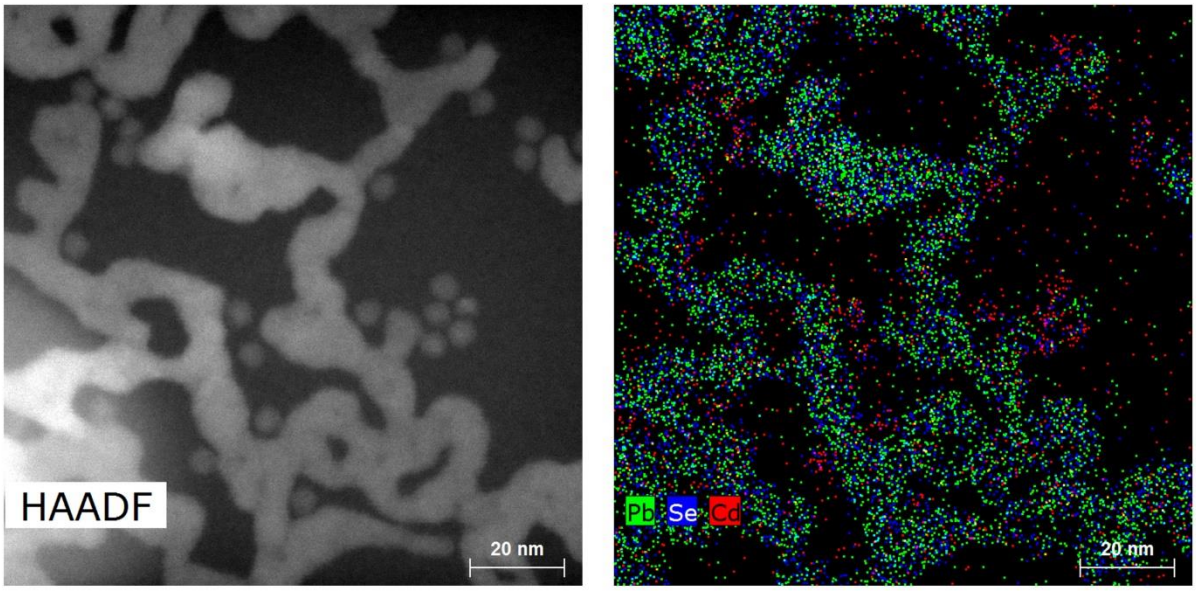

Figure 5-34: HAADF-STEM picture of a PbSe/CdSe mixture and the corresponding EDX analysis, from which it can be seen that the single nanocrystals consist mostly out of CdSe

The same analysis has been done on a different part of the same sample, to see if this part shows the same results. The HAADF picture and the corresponding atom-specific analysis are shown in Figure 5-35. Here, the difference between the superstructures and the single dots can again be clearly seen. The atom-specific analysis shows again that those single dots are made of CdSe, whereas the superstructures are made of PbSe. This shows that the CdSe is indeed not incorporated in the PbSe superstructures, but that it stays close to those superstructures.

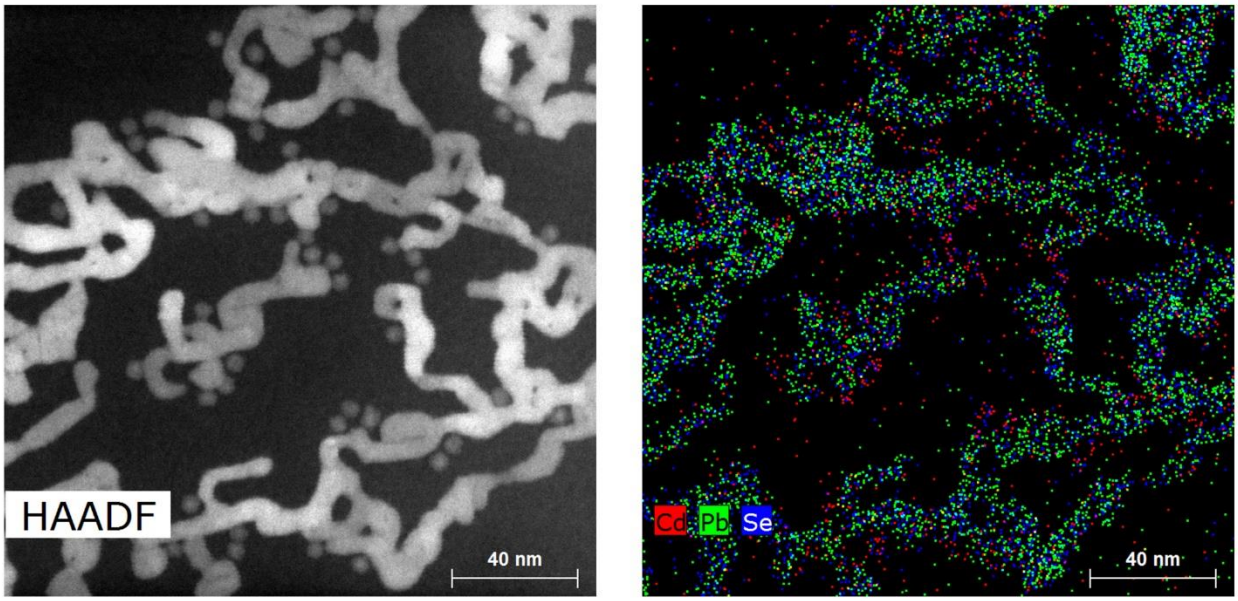

Figure 5-35: HAADF-STEM picture of a PbSe/CdSe mixture on another part of the sample and the corresponding atom-specific analysis, showing again that the single nanocrystals consist mostly out of CdSe

Using a combination of TEM, EDX, HAADF-STEM and atom-specific analysis it has been shown that CdSe does not perform oriented attachment, as expected. It will however perform self-assembly. When a mixture of PbSe and CdSe is analysed, it is seen that the PbSe will perform oriented attachment, but the CdSe will be deposited directly next to the superstructures and not in the spaces between the superstructures. This indicates that the CdSe has performed self-assembly together with the PbSe, but that the CdSe dots were left out in the oriented attachment process. This indicates that the forces that play a role in the oriented attachment are fundamentally different than those in the self-assembly. Furthermore, the forces in the self-assembly do not exclude the CdSe nanocrystals whereas the forces in the oriented attachment do exclude CdSe nanocrystals.

6. Conclusions

The goal of this Master's thesis was to provide more insight in the oriented attachment process, via oriented attachment of PbSe and the attempted oriented attachment of a mixture of PbSe and CdSe.

Using the hot injection method, star-shaped PbSe nanocrystals were synthesised. Spherical nanocrystals were needed for the oriented attachment experiments, which is the reason that nanocrystals synthesised by Joep Peters were used in this thesis. The size and shape of the PbSe nanocrystals was be characterised using UV-VIS absorption spectroscopy and Transfer Electron Microscopy (TEM). Using these techniques, and the method as explained by Moreels *et al.*[53] it was found that the used nanocrystals had a diameter of 5.5 nm, were monodisperse and had indeed a spherical shape.

CdSe particles of the same size and shape as the PbSe nanocrystals were synthesised via cation exchange on the PbSe nanocrystals as explained in section 3.3. The concentration and conversion rate of Cd was measured using ICP-OES, where it was found that the concentration is $1.15*10^{-6}$ M, the yield is 13.5% and that the conversion rate was 92%.

Oriented attachment was successful with PbSe nanocrystals using the reaction conditions as explained by Evers *et al.*[5] and Boneschanscher *et al.*[6] Furthermore, it was found that reaction conditions like the temperature, toluene volume and added surfactants have a big influence on the process.

Large patches of square superstructures have been readily synthesised in a toluene solution on an ethylene glycol substrate via this reaction procedure. It is also possible to synthesise honeycomb superstructures via oriented attachment, by doubling the amount of toluene that is used in the experiment whilst halving the concentration of nanocrystals, leading to the same amount of nanocrystals but a slower evaporation of toluene. These honeycomb superstructures are however not as large as the square superstructures and there are other superstructures present, like linear and zigzag-like superstructures. These are also found together with the square superstructures, but are not as abundant.

These results lead to the conclusion that the superstructures that are made are dependent on the concentration of PbSe nanocrystals and the amount of toluene that is used in the experiment. This is because the nanocrystals will be able to stick to the toluene/air surface with their <111> facets[5], which assembles the nanocrystals in a way that makes it favourable to form honeycombs. With a lower toluene volume, the nanocrystals stick to the ethylene glycol/toluene surface, self-assembling in square structures.

The CdSe nanocrystals were found to perform self-assembly, but they perform no attachment. When they are mixed with PbSe, it has been seen that the PbSe performs oriented attachment, but that the CdSe nanocrystals are left out in the superstructures. They are positioned however directly next to the superstructures, indicating that there must be an interaction with the PbSe nanocrystals before the attachment takes place (see section 3.4.2). It leads to the conclusion that the CdSe nanocrystals do perform self-assembly together with the PbSe nanocrystals, but that they are left out as soon as the attachment starts. This leads to the conclusion that the forces that play a role in the self-assembly are different from those that play a role in the oriented attachment.

7. Outlook

This thesis has provided new insights in the oriented attachment process, by providing information about the formation of honeycombs, which is dependent on the toluene volume, and the oriented attachment of PbSe and CdSe nanocrystals, which indicates different forces playing a role in the self-assembly and oriented attachment processes. However, more information is needed to get a complete picture in both cases.

To get more insight in the formation of honeycomb PbSe nanocrystal superstructures, more oriented attachment experiments need to be done with different reaction conditions. For example, the temperature could be varied (under room temperature) or even more solution volume could be used for a slower evaporation of toluene. This leads to a better route for the synthesis of honeycomb superstructures and hopefully eventually leads to better superstructures.

More experiments should be done with CdSe as well. Since the superstructures of PbSe were molten, the same experiment should be repeated to see if the same results are found when the structures are not molten. When this is the case, different reaction conditions (focussing on the reaction time) should be done to see the effect on the CdSe nanocrystals and to find which forces play a role in the process.

Cation exchange can be performed on the CdSe nanocrystals to change them back into PbSe. Using these PbSe nanocrystals, oriented attachment experiments should be done, to see if those nanocrystals are still able to perform oriented attachment. The nanocrystals can also be analysed using UV-VIS absorption spectroscopy and TEM to analyse the size and morphology of the nanocrystals.

8. Acknowledgements

I would like to thank my daily supervisor, Carlo van Overbeek, for all the help and discussions during this thesis. I would also like to thank Daniël Vanmaekelbergh for giving me the opportunity to do my thesis at his group. Furthermore, I would like to thank Joep Peters for allowing me to use his PbSe nanocrystals. I also would like to thank the rest of the attachment group for the input and useful discussions we had during our meetings. I would like to thank Hans Ligthart and Peter van den Beld for their help on the lab and with the gloveboxes. For his help with the TEM and EDX measurements, I would like to thank Hans Meeldijk. At last, I would like to thank all the staff members and especially the students for all our discussions and the great time I had during this thesis.

Bibliography

1. Yin, Y. & Alivisatos, A. P. Colloidal nanocrystal synthesis and the organic-inorganic interface. *Nature* **437,** 664–670 (2005).

2. Penn, R. Lee. Banfield, J. F. Oriented attachment and growth, twinning, polytypism, and formation of metastable phases: Insights from nanocrystalline TiO2. *Am. Mineral.* **83,** 1077–1082 (1998).

3. Cho, K. S., Talapin, D. V., Gaschler, W. & Murray, C. B. Designing PbSe nanowires and nanorings through oriented attachment of nanoparticles. *J. Am. Chem. Soc.* **127,** 7140–7147 (2005).

4. Chang, S. An all-nanocrystal transistor emerges from solution. *Phys. Today* **69,** 17–19 (2016).

5. Evers, W. H. *et al.* Low-dimensional semiconductor superlattices formed by geometric control over nanocrystal attachment. *Nano Lett.* **13,** 2317–2323 (2013).

6. Boneschanscher, M. P. *et al.* Long-range orientation and atomic attachment of nanocrystals in 2D honeycomb superlattices. *Science (80-.).* **344,** 1377–1380 (2014).

7. de Mello Donegá, C. & De Groot, F. Advanced spectroscopy of nanomaterials. *Lectures* (2015).

8. Alivisatos, A. P. Perspectives on the Physical Chemistry of Semiconductor Nanocrystals. **3654,** 13226–13239 (1996).

9. de Mello Donegá, C. Synthesis and properties of colloidal heteronanocrystals. *Chem. Soc. Rev.* **40,** 1512–46 (2011).

10. Murray, C. B., Noms, D. J. & Bawendi, M. G. Synthesis and Characterization of Nearly Monodisperse CdE (E=S, Se, Te) Semiconductor Nanocrystallites. *J. Am. Chem. Soc.* **115,** 8706–8715 (1993).

11. Finney, E. E. & Finke, R. G. Nanocluster nucleation and growth kinetic and mechanistic studies : A review emphasizing transition-metal nanoclusters ☆. **317,** 351–374 (2008).

12. De Mello Donegá, C., Liljeroth, P. & Vanmaekelbergh, D. Physicochemical evaluation of the hot-injection method, a synthesis route for monodisperse nanocrystals. *Small* **1,** 1152–1162 (2005).

13. Hassinen, A. *et al.* Short-Chain Alcohols Strip X-Type Ligands and Quench the Luminescence of PbSe and CdSe Quantum Dots, Acetonitrile Does Not.pdf. *J. Mater. Chem.* **134,** (2012).

14. Groeneveld, E. Synthesis and optical spectroscopy of (hetero) -nanocrystals : An exciting interplay between chemistry and physics. (2012).

15. Beberwyck, B. J., Surendranath, Y. & Alivisatos, A. P. Cation Exchange : A Versatile Tool for Nanomaterials Synthesis. (2013).

16. Casavola, M. *et al.* Anisotropic Cation Exchange in PbSe/CdSe Core/Shell Nanocrystals of Different Geometry. (2012).

17. Rivest, J. B. Cation exchange on the nanoscale: an emerging technique for new

material synthesis, device fabrication, and chemical sensing. 89–96 (2013). doi:10.1039/c2cs35241a

18. Dong, A., Chen, J., Vora, P. M., Kikkawa, J. M. & Murray, C. B. Binary nanocrystal superlattice membranes self-assembled at the liquid – air interface. *Nature* **466,** 474–477 (2010).

19. Murray, C. B. Synthesis and Characterization of Monodisperse Nanocrystals and Close-Packed Nanocrystal Assemblies. 545–610 (2000).

20. Vanmaekelbergh, D. Self-assembly of colloidal nanocrystals as route to novel classes of nanostructured materials. *Nano Today* **6,** 419–437 (2011).

21. Rogach, A. L. *et al.* Organization of matter on different size scales: Monodisperse nanocrystals and their superstructures. *Adv. Funct. Mater.* **12,** 653–664 (2002).

22. Heath, J. R. Materials science: Synergy in a superlattice. *Nature* **445,** 492–493 (2007).

23. Bigioni, T. P. *et al.* Kinetically driven self assembly of highly ordered nanoparticle monolayers. *Nat. Mater.* **5,** 265–270 (2006).

24. Podsiadlo, P., Krylova, G. V., Demortière, A. & Shevchenko, E. V. Multicomponent periodic nanoparticle superlattices. *J. Nanoparticle Res.* **13,** 15–32 (2011).

25. Goodfellow, B. W., Yu, Y., Bosoy, C. A., Smilgies, D. & Korgel, B. A. The Role of Ligand Packing Frustration in Body-Centered Cubic (bcc) Superlattices of Colloidal Nanocrystals. (2015). doi:10.1021/acs.jpclett.5b00946

26. Hapiuk, D. *et al.* Oriented Attachment of ZnO Nanocrystals. (2013).

27. Ziherl, P. & Kamien, R. D. Maximizing Entropy by Minimizing Area : Towards a New Principle of Self-Organization. **105,** (2001).

28. Soligno, G., Dijkstra, M. & Van Roij, R. Self-Assembly of Cubes into 2D Hexagonal and Honeycomb Lattices by Hexapolar Capillary Interactions. *Phys. Rev. Lett.* **116,** 1–5 (2016).

29. Thapar, V., Hanrath, T. & Escobedo, F. A. Entropic self-assembly of freely rotating polyhedral particles confined to a flat interface. *Soft Matter* **11,** 1481–1491 (2015).

30. van Rijssel, J. *et al.* Enthalpy and entropy of nanoparticle association from temperature-dependent cryo-TEM. *Phys. Chem. Chem. Phys.* **13,** 12770–12774 (2011).

31. Choi, J. J., Bian, K., Baumgardner, W. J., Smilgies, D. & Hanrath, T. Interface-Induced Nucleation, Orientational Alignment and Symmetry Transformations in Nanocube Superlattices. (2012).

32. Talapin, D. V., Shevchenko, E. V., Murray, C. B., Titov, A. V. & Král, P. Dipole - Dipole interactions in nanoparticle superlattices. *Nano Lett.* **7,** 1213–1219 (2007).

33. Kortschot, R. J., Van Rijssel, J., Van Dijk-Moes, R. J. A. & Erné, B. H. Equilibrium structures of PbSe and CdSe colloidal quantum dots detected by dielectric spectroscopy. *J. Phys. Chem. C* **118,** 7185–7194 (2014).

34. Klokkenburg, M. *et al.* Dipolar structures in colloidal dispersions of PbSe and CdSe quantum dots. *Nano Lett.* **7,** 2931–2936 (2007).

35. Boles, M. A. & Talapin, D. V. Many-Body Effects in Nanocrystal Superlattices:

Departure from Sphere Packing Explains Stability of Binary Phases. *J. Am. Chem. Soc.* **137,** 4494–4502 (2015).

36. Kaushik, A. P. & Clancy, P. Solvent-driven symmetry of self-assembled nanocrystal superlattices - A computational study. *J. Comput. Chem.* **34,** 523–532 (2013).

37. Choi, J. J. *et al.* Controlling nanocrystal superlattice symmetry and shape-anisotropic interactions through variable ligand surface coverage. *J. Am. Chem. Soc.* **133,** 3131–3138 (2011).

38. Nagaoka, Y., Chen, O., Wang, Z. & Cao, Y. C. Structural control of nanocrystal superlattices using organic guest molecules. *J. Am. Chem. Soc.* **134,** 2868–2871 (2012).

39. Penn, R. L. & Banfield, J. F. Imperfect oriented attachment: Dislocation generation in defect-free nanocrystals. *Science (80-.).* **281,** 969–971 (1998).

40. Zhang, Q., Liu, S.-J. & Yu, S.-H. Recent advances in oriented attachment growth and synthesis of functional materials: concept, evidence, mechanism, and future. *J. Mater. Chem.* **19,** 191 (2009).

41. Zhang, J. *et al.* A Multistep Oriented Attachment Kinetics: Coarsening of ZnS Nanoparticle in Concentrated NaOH. *J. Am. Chem. Soc.* **128,** 12981–12987 (2006).

42. Penn, R. L. & Banfield, J. F. Morphology development and crystal growth in nanocrystalline aggregates under hydrothermal conditions: Insights from titania. *Geochim. Cosmochim. Acta* **63,** 1549–1557 (1999).

43. Pacholski, C., Kornowski, A. & Weller, H. Self-assembly of ZnO: From nanodots to nanorods. *Angew. Chemie - Int. Ed.* **41,** 1188–1191 (2002).

44. Zitoun, D., Pinna, N., Frolet, N. & Belin, C. Single crystal manganese oxide multipods by oriented attachment. *J. Am. Chem. Soc.* **127,** 15034–15035 (2005).

45. Yansong, X. & Zhiyong, T. Role of self-assembly in construction of inorganic nanostructural materials. *Sci. China Chem.* **55,** 2272–2282 (2012).

46. Dalmaschio, C. J., Ribeiro, C. & Leite, E. R. Impact of the colloidal state on the oriented attachment growth mechanism. *Nanoscale* **2,** 2336–2345 (2010).

47. Liao, H., Cui, L., Whitelam, S. & Zheng, H. Real-time imaging of Pt$_3$Fe nanorod growth in solution. *Science (80-.).* **336,** 1011–1014 (2012).

48. Rupich, S. M. & Talapin, D. V. Colloidal self-assembly: Interlocked octapods. *Nat. Mater.* **10,** 815–816 (2011).

49. Banfield, J. F., Welch, S. A., Zhang, H., Ebert, T. T. & Penn, R. L. Oxyhydroxide Biomineralization Products Aggregation-Based and in Growth Microstructure Natural Development Iron Oxyhydroxide Biomineralization Products. **289,** 751–754 (2000).

50. Pietryga, J. M. *et al.* Utilizing the Lability of Lead Selenide to Produce Heterostructured Nanocrystals with Bright , Stable Infrared Emission. 4879–4885 (2008).

51. Geyter, B. De, Hens, Z., Geyter, B. De & Hens, Z. The absorption coefficient of PbSe / CdSe core / shell colloidal quantum dots Advertisement : The absorption coefficient of PbSe / CdSe core / shell colloidal quantum dots. **161908,** 42–45 (2010).

52. Houtepen, A. J., Koole, R., Meeldijk, J. & Hickey, S. G. The Hidden Role of Acetate in the PbSe Nanocrystal Synthesis. 6792–6793 (2006).

53. Moreels, I. *et al.* Composition and Size-Dependent Extinction Coefficient of Colloidal PbSe Quantum Dots. *Chem. Mater.* **19,** 6101–6106 (2007).

54. Landry, M. L., Morrell, T. E., Karagounis, T. K., Hsia, C. H. & Wang, C. Y. Simple syntheses of CdSe quantum dots. *J. Chem. Educ.* **91,** 274–279 (2014).

55. Groeneveld, E. *et al.* Tailoring ZnSe-CdSe colloidal quantum dots via Cation Exchange: From core/shell to alloy nanocrystals. *ACS Nano* **7,** 7913–7930 (2013).

56. Holzwarth, U. & Gibson, N. The Scherrer equation versus the 'Debye-Scherrer equation'. *Nat. Nanotechnol.* **6,** 534–534 (2011).

57. Ball, D. W. *Physical Chemistry*. (Brooks/Cole Cengage Learning, 2003).

9. Appendices

Appendix A: Details of the nanocrystals mentioned in this thesis

Quantum dots	Size (nm)	Solvent	Concentration (M)
PbSe[a]	5.5[b]	Toluene	$2*10^{-4}$ [d]
CdSe	5.5[c]	Toluene	$1.15*10^{-6}$ [e]

a) Synthesised by Joep Peters
b) Size measured using UV-VIS absorption spectrometer
c) Assumed to be the same size as PbSe
d) Determined using UV-VIS absorption spectrometer
e) Determined using ICP, using the ratio with PbSe

Appendix B: Determination of crystal facets using electron diffraction

It is possible to determine the nanocrystal orientation using an electron diffractogram (ED). This is because electrons in the beam only scatter from crystal planes that stand parallel to the incoming electron beam of the TEM. The investigated superstructures are singly ordered nanocrystals that have one alignment, this makes it possible to determine the facets that stand perpendicular to the substrate. The Miller indices of the facets can be calculated using equation B-1.[57]

$$Constant = \frac{\#\ pixels}{h^2+k^2+l^2} \qquad \text{(B-1)}$$

The # pixels is the amount of pixels between two opposite ED spots. The Miller indices are defined by h, k and l.

The planes that scatter are defined by the crystal structure. This is because scattering is only allowed if the structure factor of a nanocrystal is not zero. The PbSe nanocrystals used in this thesis have the FCC (face-centered cubic) structure and so do the cation exchanged CdSe nanocrystals. This means that only Miller indices that are all odd or all even have a structure factor that is not zero.

Using the length measured in pixels between two ED spots in the same 'ring' and specific miller indices, the corresponding facets can be calculated, as seen in Figure 9-1.

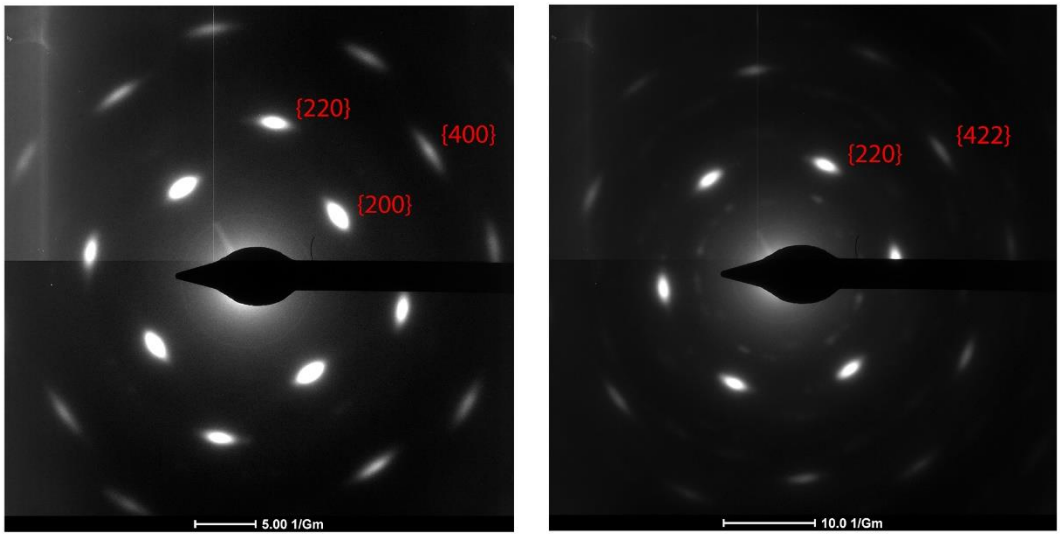

Figure 9-1: Electron diffractogram pictures with the corresponding Miller indices